MICROCOPY RESOLUTION TEST CHART
NATIONAL BUREAU OF STANDARDS-1963

②

Stability of the Slope of an Embankment Constructed at Washington National Airport

Deborah J. Armstrong, P.E.
U.S. MILLER, CAPT, FA ?
200 Stovall Street
Alexandria, VA 22332

88 1 29 090

REPORT DOCUMENTATION PAGE		READ INSTRUCTIONS BEFORE COMPLETING FORM
1. REPORT NUMBER	2. GOVT ACCESSION NO.	3. RECIPIENT'S CATALOG NUMBER
4. TITLE *(and Subtitle)* Stability of the Slope of an Embankment Constructed at Washington National Airport		5. TYPE OF REPORT & PERIOD COVERED Final Report; 16 OCT 87
		6. PERFORMING ORG. REPORT NUMBER
7. AUTHOR(s) Deborah L. Nykyforchyn		8. CONTRACT OR GRANT NUMBER(s)
9. PERFORMING ORGANIZATION NAME AND ADDRESS Student, HQDA, MILPERCEN (DAPC-OPA-E), 200 Stovall Street, Alexandria, VA 22332		10. PROGRAM ELEMENT, PROJECT, TASK AREA & WORK UNIT NUMBERS
11. CONTROLLING OFFICE NAME AND ADDRESS HQDA, MILPERCEN, ATTN: (DAPC-OPA-E) 200 Stovall Street, Alexandria, VA 22332		12. REPORT DATE 16 OCT 87
		13. NUMBER OF PAGES 95
14. MONITORING AGENCY NAME & ADDRESS *(If different from Controlling Office)*		15. SECURITY CLASS. *(of this report)* Unclassified
		15a. DECLASSIFICATION DOWNGRADING SCHEDULE

16. DISTRIBUTION STATEMENT *(of this Report)*

Approved for public release; distribution is unlimited.

17. DISTRIBUTION STATEMENT *(of the abstract entered in Block 20, If different from Report)*

18. SUPPLEMENTARY NOTES

Thesis, Master of Science in Civil Engineering; The Johns Hopkins University, Baltimore, MD.

19. KEY WORDS *(Continue on reverse side if necessary and identify by block number)*

Embankment stability; slope stability; finite element analysis of slope stability; geotextile reinforced slope

20. ABSTRACT *(Continue on reverse side if necessary and identify by block number)*

The stability of an earthen embankment supporting the overrun of Runway 18 at Washington National Airport was examined using the finite element method. The purpose of this work was to study the applicability of the finite element method to the design of embankments. The embankment is partially submerged, layered and reinforced with a geotextile. The embankment was designed

DD ₁ FORM 73 **1473**   EDITION OF 1 NOV 65 IS OBSOLETE

Stability Analysis of the Slope of an Embankment

Constructed at Washington National Airport

by

Deborah L. Nykyforchyn

A dissertation submitted to The Johns Hopkins University

in conformity with the requirements for the degree of

Master of Science in Engineering

Baltimore, Maryland

1987

ABSTRACT

The stability of the slope of an earthen embankment supporting the overrun of Runway 18 at Washington National Airport was examined using the finite element method. The purpose of this work was to study the applicability of the finite element method to the design of the slopes of embankments. The embankment is partially submerged, layered and reinforced with a geotextile. The embankment was designed by the Baltimore District of the U.S. Army Corps of Engineers based upon analysis results obtained using the simplified Bishop method- a version of the method of slices which is widely used for estimating the stability of slopes.

Finite element analyses were conducted considering the embankment with and without a reinforcing geotextile. The factors of safety obtained using the finite element method were compared with those obtained using the simplified Bishop method. Additionally, the development of failure within the embankment and the deformations of the embankment at failure were studied.

The finite element method was found to be capable of providing physically reasonable descriptions of the behavior of embankment slopes. Fair agreement was observed between the corresponding factors of safety obtained using the simplified Bishop method and the finite element method. The finite element method resulted in higher

factors of safety. However, difficulty was encountered in precisely defining the state of failure.

It was concluded that the finite element method can provide refined estimates of behavior for complex problems but may require considerable effort, cost, and expertise. As a result, this method would appear best suited for later stages in the design of critical facilities.

Several areas toward which future work could be directed were identified. Work in these areas would be intended to advance the ability of the finite element method to describe the behavior of embankment slopes. These areas include more precise definitions of the state of failure, more realistic modeling of soil behavior, use of effective stress analysis, accounting for partial dissipation of pore water pressures and the development of boundary conditions which can describe more effectively the behavior of regions surrounding the region of interest.

ACKNOWLEDGMENTS

TABLE OF CONTENTS

LIST of TABLES

LIST OF ILLUSTRATIONS

Notation

b = width of slice

$[D]_e$ = elasticity (material) or constitutive matrix

c = cohesion

c_i = equivalent cohesive strength of geotextile layer, unit cohesion of geotextile

c_u = unit cohesion of soil

d = displacement

$[D]$ = differential operators matrix

D = depth ratio

$\{\epsilon\}_e$ = element strain vector

E = normal force on vertical face of slice, modulus of elasticity

$\{f\}_e$ = element body force vector

FEM = finite element method

FS = trial factor of safety

H = height

ΔH = increment of height

h = height of slice; thickness foundation layer

h_e = thickness of element

$[K^{(e)}]$ = element stiffness matrix

k_0 = effective coefficient of earth pressure at rest

L_f = length of failure arc in foundation soil beneath geotextile

N = total stability number

N_f	=	stability number for geotextile
N_u	=	stability number for foundation
P	-	normal force on base of slice
P'	-	effective normal force on base of slice
S	-	shear force on base of slice
s	-	shear strength
$\{t\}_e$	=	element traction vector
T	-	shear force on vertical face of slice
T_f	=	tensile strength of geotextile
u_h	=	hydrostatic pore water pressure
u_s	=	pore water pressure in excess of hydrostatic pressure
W	-	total weight of slice
W_1	=	weight of portion of slice above water table
W_2	=	submerged weight of portion of slice below water table
z	-	depth of water below water table; depth to base of slice below water table
α	=	angle between base of slice and horizontal
ε	=	normal strain
$\varepsilon_x, \varepsilon_y$	=	lateral normal strains in x and y directions, respectively
ε_z	=	axial normal strain in z direction
$\Delta\varepsilon$	=	increment of normal strain in direction of normal stress, $\Delta\sigma$
ϕ	-	angle of internal friction (degrees)
γ	=	total unit weight of soil layer above water table; unit weight
γ'	=	effective unit weight of soil layer below the water table

xi

γ_h -   unit weight of embankment material

γ_{sat} -   saturated unit weight

γ_w -   unit weight of water

Γ^e -   element boundary

$\Pi(d)$ - potential energy functional

σ -   normal stress

$\Delta\sigma$ -   increment of normal stress

σ_f -   von Mises failure stress of the material

σ_h -   average lateral stress

$\sigma_{x,y,z}$ -   principal stresses in x, y, and z directions, respectively

σ_z -   axial normal stress in z direction at failure

$(\sigma)_e$ -   element stress vector

τ -   shear stress

υ -   Poisson's Ratio

Ω^e -   element domain

$[\Psi]_e$ -   element interpolation functions matrix

CHAPTER 1
INTRODUCTION

1.1 Introduction

In this chapter the objective and the purpose of the work described herein are discussed. The organization of this thesis is also presented.

1.2 Objective

The objective of the work described herein was to carry out finite element analyses (see Chapter 4) for a partially submerged, layered, earthen embankment with and without a reinforcing geotextile (a thin, flexible, porous sheet of fibrous plastic). The results obtained from the finite element analyses were to be compared with results obtained using the simplified Bishop method (see Chapter 4), a method of analysis often used for estimating the stability of slopes. The progressive development of the failure of the slope of the embankment and the deformation of the embankment at failure were to be studied.

1.3 Purpose

The purpose of the study reported in this thesis was to investigate the applicability of finite element analysis to the design of

the slopes of partially submerged, layered earthen embankments reinforced with geotextiles. Analyses currently used (for example, the simplified Bishop method) offer ease of usage. However, in some cases, such analyses may not be as detailed as is desirable, leading to uncertainty with respect to slope stability. The finite element method may be quite representative of the embankment slope of interest. This method may permit the modeling of complex geometry, material behavior, and loading. This method may be capable of accurately describing such items as the progressive development of failure and the deformation at failure. As a result of its potential for material behavior descriptiveness, the finite element method may lead to less uncertainty in the design of the slopes of embankments.

1.4 Organization

Chapter 2 provides a discussion of relevant literature. Chapter 3 provides information on the embankment of interest at Washington National Airport. Chapter 4 provides a summary of the simplified Bishop method and the finite element method as applied to embankments. In Chapter 5 the results from comparable analyses conducted using these two methods are presented and discussed. In Chapter 6 conclusions and suggestions for future work are presented.

Chapter 2
Review of Literature

2.1 Introduction

In this chapter, literature is discussed which relates to estimating the stability of slopes on layered deposits reinforced with geotextiles.

2.2 Literature Review

Various analysis methods have been developed for estimating the stability of slopes. The method of slices (see Chapter 4) was developed by Fellenius [28]. Basically, in the method of slices, a continuous, arc-shaped, potential failure surface across the slope is assumed. The potential sliding mass above this surface is divided into vertical slices. Conditions of equilibrium are imposed and factor of safety against sliding estimated.

In the method of slices it is assumed that the slope consists of an ideal plastic (perfectly plastic) material. An ideal plastic material has a defined yield stress. Failure is assumed to occur simultaneously along the selected arc-shaped surface. A trial factor of safety is calculated for the selected surface.

Several appropriate surfaces are examined to determine the smallest trial factor of safety for a given slope. The smallest trial

factor of safety is considered to be the best estimate of the factor of safety. The corresponding surface is considered to represent the most probable failure surface of the slope. Other investigators, for example, Bishop [2], and Morgenstern and Price [20] refined the method of slices to account for such items as interslice forces.

As a result of assumptions, analyses based on the method of slices may only provide rough estimates of the factor of safety and failure surface [5]. Assumptions that are likely to cause significant errors include the assumption of an arc-shaped failure surface, and simultaneous failure along the failure arc. Sowers [28] and Terzaghi and Peck [31] pointed out that in slopes on layered soil deposits failure surfaces generally pass through the weakest soil layers along interfaces. Thus, in such deposits the shapes of actual failure surfaces may be highly irregular. Additionally, failures are usually progressive. Frohlich [5] indicated that local failures often occur at isolated locations within a slope prior to overall failure. Overall failure of the slope occurs when these local failure zones merge to form a continuous failure surface. Such details are not considered in the method of slices.

The finite element method (see Chapter 4) has the ability to account for most of the important items discussed above. The method has been used in a number of previous studies concerning the behavior of slopes (see, for example, Lo and Lee [16], Naylor [21] and Hoeg [10]).

The finite element method is a powerful numerical technique of solving well-posed boundary value problems. To date the method has been used to solve a variety of problems. a detailed discussion is beyond the scope of this thesis

The finite element method involves dividing an appropriate region of interest into small regions called elements. In the standard finite element method, the elements are inter-connected at discrete points known as nodes. Displacements at these nodes then form the primary unknowns to be determined. Secondary variables, such as stresses are derived from the displacements. Within each element the displacements are assumed to vary in a certain manner. The variation is represented by mathematical functions known as shape functions (e.g. linear, quadratic, etc). The primary unknowns are determined by employing a suitable stationary principle.

Minimization of the total potential energy functional over the domain, after the imposition of boundary conditions, results in a set of linear algebraic equations for the unknowns. This matrix equation is then solved using one of the standard methods of solving a system of linear simultaneous equations.

Material properties and boundary conditions are defined for the elements and the loading of the embankment is simulated Conditions of equilibrium are imposed The finite element method may represent the embankment slope quite well For example, the progressive nature of the failure of a slope and irregular failure surfaces may be described. Using the finite element analyses one can describe

nonlinear stress-strain behavior. Also complex geometries and loading sequences may be described. Actual embankment slopes which failed have been analytically modeled using finite element methods. The embankment models were loaded to failure. The finite element method was found to closely predict the zones of failure and factors of safety [14].

Both the method of slices and finite element method have been used to model embankments reinforced with geotextiles. A geotextile is a thin, flexible, porous sheet of fibrous plastic. Basically, geotextiles act as tension members. Using the method of slices, Fowler [6] considered the resistance provided by a geotextile as additional soil cohesion. Leshchinsky [17] considered this resistance as an additional moment resisting movement of the slope. Using the finite element method, Rowe [26] modeled a geotextile as an additional thin layer. In each case, the geotextile was found to lead to an increase in the factor of safety, as expected.

The author is not aware of any publication which presents comparisons between results obtained using the method of slices and finite element analysis to predict the behavior of partially submerged, layered, embankments reinforced with geotextiles.

CHAPTER 3
CASE STUDY

3.1 Introduction

In this chapter, relevant information concerning the design of the safety overrun for Runway 18 of the Washington National Airport is briefly summarized. A background is given, after which site conditions, the final design concept and critical design conditions are discussed. Details may be found in Reference 27.

3.2 Background

The Washington National Airport is located adjacent to the Potomac River in Alexandria, Virginia. Land reclaimed from the Potomac River was used for the landing field. The base for the facility was constructed by pumping sand and gravel from the Potomac River into a region surrounded by a dike [27].

In 1978, The Federal Aviation Administration (FAA) identified the existing safety overrun area for Runway 18 as being insufficient under existing guidelines. In 1979 the FAA commissioned the Baltimore District of the U.S. Army Corps of Engineers to design and manage construction of a runway overrun [19]. This extension was to be an earthen embankment covering an area approximately 700 feet long by 600 feet wide (7 acres) as shown in Figure 3.1 [19].
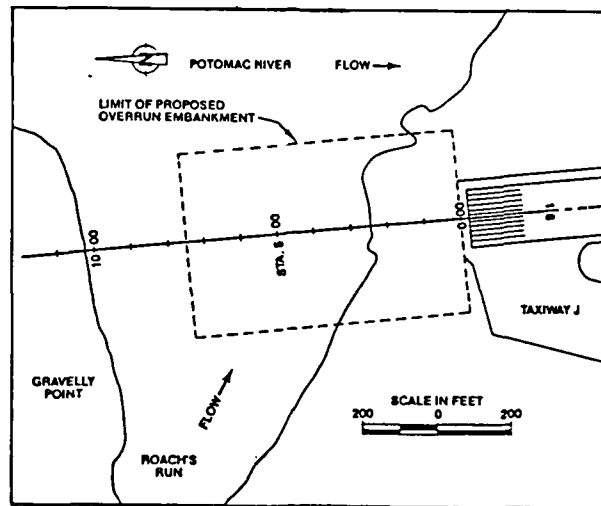
Figure 3.1 Location of Proposed Embankment

3.3 Site Conditions

Several major geotechnical obstacles to an embankment were encountered. Those relevant to the work described herein included the submergence of the proposed construction site by six to seven feet of water and a foundation of soft, highly plastic, silts and clays [27]. The foundation soils were judged to be inadequate for supporting the proposed embankment based on extensive geotechnical subsurface exploration.

An extensive geotechnical subsurface exploration was conducted to define subsurface conditions. A total of thirty-three soil borings were drilled. Standard penetration tests were conducted in all

bore holes, while undisturbed samples were obtained for laboratory testing. Field vane shear tests were conducted at eight bore holes [27].

A laboratory testing program was developed to determine various properties of the soil layers. Compaction tests, triaxial shear tests, unconfined compression tests, consolidation tests, and standard classification tests were conducted.

A cross-section, showing typical layering at the site, based on the field and laboratory test data, is shown in Figure 3.2 [19].
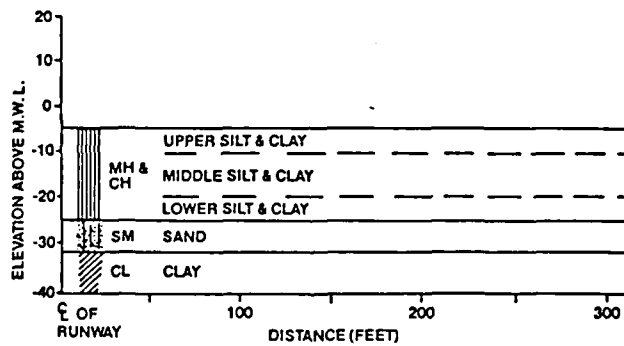
Figure 3.2 Cross Section Typical of Site

The upper layers of soil were found to be primarily soft silts (MH) and highly plastic clays (CH), and silty sands (SM).

Relevant properties of the upper layers, inferred from the laboratory and field tests, are shown in Table 3.1 [27].

Soil Type	γ(sat) (pcf)	Shear Strength			
		U-U(Q) Avg.		U-U (Q) Min.	
		φ	c (psf)	φ	c (psf)
Upper Silt & Clay	90	0	100	0	50
Middle Silt & Clay	90	0	200	0	150
Lower Silt & Clay	90	0	250	0	200
Sandy Silt	120	32	0	32	0
Clay	115	0	1000	0	1000

Table 3.1 Relevant Soil Data for Site

The saturated densities of the silt and clay layers, considered to be the most critical layers, with respect to the sandy silt and clay layers, ranged from approximately 80 to 100 pcf and the cohesive shear strengths of these layers ranged from 50 psf near the mudline to 400 psf at isolated locations. Values of cohesive strength were typically between 100 and 250 psf. In-situ vane shear tests indicated high sensitivity of the upper silt and clay layers to disturbance. These soils were found to lose 50% to 80% of their strength as a result of remolding [18,19, 27].

3.4 Final Design Concept

Various design concepts, directed at eliminating the problems created by the soft upper layers, were considered. The Baltimore District of the Corps of Engineers concluded that, given the soil conditions and available technology, the most effective means for

providing an adequate foundation for the runway safety overrun would be to place a reinforcing geotextile over the existing soft soils.

The American Society for Testing and Materials (ASTM) identifies a geotextile as:

> any permeable textile material used with foundation, soil, rock, or any geotechnical related material, that is an integral part of a man-made project, structure or system [23].

Geotextiles are the largest group of geosynthetics. Modern geotextiles are referred to by a variety of names: filter fabrics, engineering fabrics, geofabrics, and drainage fabrics. A detailed discussion of geotextile properties, manufacturing processes, and functions are provided by Koerner [14], Rankilor [23], and Van Zanten [32].

With a geotextile in place, granular and random soil could be placed on the geotextile to create an embankment which would support the runway overrun.

The reinforcing geotextile offered several features. The geotextile, with its high strength, could prevent failures of the slopes of the embankment, excessive vertical displacements of the embankment, and lateral sliding of the embankment. The geotextile could also separate the embankment fill from the underlying soft material thus preventing penetration of the fill into the underlying material.

3.5 Critical Design Conditions

Both the end-of-construction and sudden drawdown (rapid drop in the level of surrounding water) conditions were considered by the Corps of Engineers as critical to the design of stable slopes. The end-of-construction condition was considered to be more critical by the Corps of Engineers. As a result. only the end-of-construction condition was considered in the work presented herein.

Failure at the end-of-construction would be expected to occur within the slopes of the embankment as a result of unbalanced net applied gravity loads. For the modeling of the end-of-construction, condition it was assumed that the embankment had been constructed but that no consolidation of the foundation silt and clay had occurred under the loads from the embankment. This situation implies that the foundation silt and clay does not have an increase in shear strength due to consolidation. For the end-of-construction condition the minimum acceptable factor of safety was specified as 1.2.

For the sudden drawdown condition a rapid drop in the water level was considered to take place after a high tide or flooding. Under these conditions the embankment soils were considered to be totally saturated. Again, failure would be expected to occur as a result of unbalanced net applied gravity loads but the failure would be associated with the dissipation of excess pore water pressures

Chapter 4

Theory of Stability of Embankment Slopes

4.1 Introduction

In this chapter, various modes of failure of embankment slopes are discussed. Types of analyses for estimating the stability of slopes are reviewed. The simplified Bishop method, often used for estimating the stability of embankment slopes, is summarized. The Finite Element Method (FEM), used for refined estimates of the stability of embankment slopes, is discussed in some detail.

4.2 Failure of Embankment Slopes

An embankment slope is said to experience failure when a portion of the slope undergoes large movement relative to its surroundings. Failures of embankment slopes often occur along distinct surfaces. The slope of an embankment may fail in one of three possible modes (Figure 4.1) [4].

Circular   Non Circular

(a) Rotational Slips

(b) Translational Slip   (c) Compound Slip
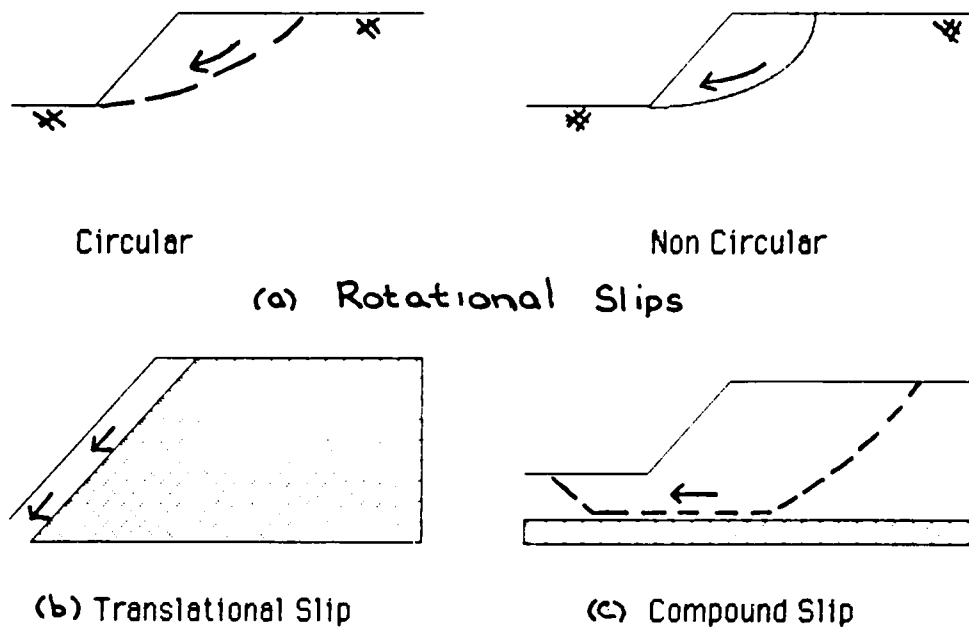
Figure 4.1   Modes of Slope Failure

The shape of the failure surface may be irregular, depending on the homogeneity of the material of the slope (Figure 4.1). If the material is homogeneous and a large circle can be formed, the most critical failure surface will be cylindrical (Figure 4.1(a)). This occurs because a circle has the least surface are per unit mass. In the case of the infinite slope with depth much smaller than length (Figure 4.1(b)), the most critical failure surface will be a plane parallel to the slope. If several planes of weakness exist, the most critical failure surface will be a series of planes passing through the weak strata. In some cases,

a combination of plane, cylindrical, and other irregular failure surfaces may exist (Figure 4.1(c)).

Failure generally occurs when the shear stress (τ), which acts along some continuous surface across the slope equals, at every point along the surface, the shear strength of the soil (s). Slope failures are generally progressive. That is, initally the shear stress may exceed the shear strength only at isolated locations along the ultimate failure surface. As the net applied load is increased, as in the case of the construction of an earthen embankment, the localized failure zone may extend, leading to overall failure. A state of limiting equilibrium is said to exist when a slope is on the verge of failure.

4.3 Types of Stability Analyses

Slope stability analyses are conducted for a slope mainly to estimate the factor of safety of the slope with respect to a failure of the slope. Two types of stability analysis may be performed, a total stress analysis and an effective stress analysis. Both are discussed below. Tezaghi and Peck [31] and Huang [11] discuss these types of analyses in modest detail.

The results presented herein are based on total stress analyses. In a total stress analysis, effective stresses and pore water pressures are not treated separately. The effects of pore water pressures on soil strength are taken into account by testing the soil samples at conditions comparable to those which are likely to prevail in the field. Total stress analyses are often used for analyzing embankments

constructed on saturated cohesive soils. The layers judged to be the most critical with respect to the stability of the slopes of the embankment analyzed herein consist of saturated cohesive soil. With such soils, the dissipation of pore water pressures resulting from loading may take considerable time. Thus, at the end-of-construction the soil may be in its weakest state and end-of-construction conditions may be critical. In this case, the appropriate strength for use in analysis would be the undrained shear strength corresponding to conditions at the end-of-construction.

In an effective stress analysis, effective stresses and pore water pressures are treated separately. Pore water pressures as well as effective strength parameters must be known to carry out an effective stress analysis.

A total stress analysis is often used for determining short-term stability during or at the end-of-construction. Total stress analysis has an advantage of not requiring additional, often costly testing procedures to determine pore water pressure. An effective stress analysis is often used for long-term stability. Three cases of long-term stability often considered by effective stress analyses are: steady-state seepage, rapid drawdown, and earthquake sites. An advantage of an effective stress analysis is knowledge of the drained shear strength of the soil.

4.4 Estimating Stability of Slopes - Simplified Bishop Method

4.4.1 General- Simplified Bishop Method

The simplified Bishop method is often used for estimating the stability of slopes [11]. The simplified Bishop method is based on the method of slices (Figure 4.2) [2]. A circular, potential failure surface is assumed. The soil mass above this surface is subdivided into vertical sections or slices. A trial factor of safety is determined by imposing the conditions of equilibruim on the mass and the slices. The forces or stresses acting on the potential failed mass are shown in Figure 4.2(a). These forces or stresses may include the weights of the soil mass and any water (W), external loads, water pressure (u_h and u_s) and shearing (S) and normal stresses (P') within the soil. The slices are assumed to have unit thickness and width b. The forces which may act on a typical slice include the normal force (P) which may include components due to effective normal stresses within the soil, hydrostatic pore water pressures (u_h) and excess pore water pressure (u_s), the shear force (S) from the soil, the total weight of the slice (W), and the shear (T) and normal (E) forces acting on the vertical faces of the slice.

(a) Slope Potential Failed Mass　　　(b) Slice
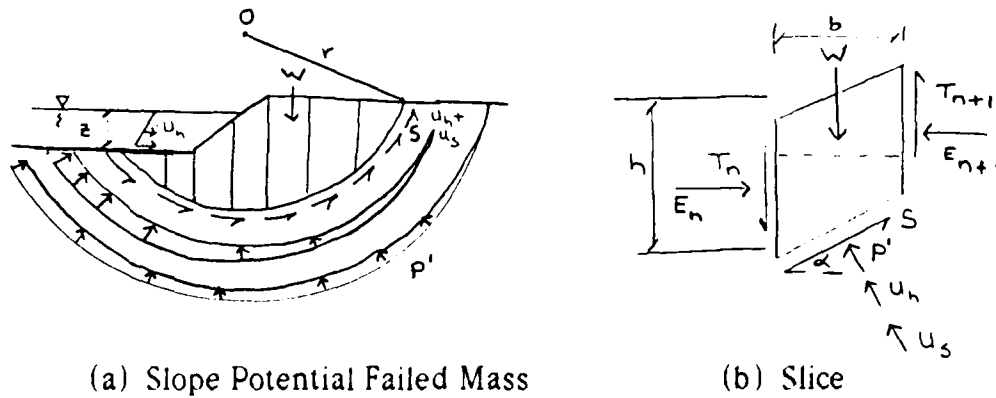
Figure 4.2 Freebody Diagrams for Potential
Failed Mass and Slice

The trial factor of safety, FS, based on the simplified Bishop method, is defined as the ratio of the resisting moment, about the center, 0, of the trial circular arc, (Figure 4.2(a)), to the net applied moment :

$$FS = \frac{\text{Resisting Moment}}{\text{Net Applied Moment}} \qquad (4.1)$$

The net applied moment tends to cause movement of the soil mass above the potential failure surface. The resisting moment tends to resist such movement. The resisting moment corresponds to the moment developed as a result of the development, along the potential failure surface, of shear stresses equaling the value of the shear strengths of the soil.

For a partially submerged slope, the trial factor of safety (FS) as defined by the simplified Bishop Method for a total stress analysis is:

$$FS = \frac{\sum [cb + (W_1 + W_2 + z\gamma_w b)\tan\phi][\sec\alpha /(1 + \tan\phi\tan\alpha /FS)]}{\sum (W_1 + W_2 + z\gamma_w b)\sin\alpha} \qquad (4.2)$$

where

c = cohesion

b = width of slice

ϕ = angle of internal friction (degrees)

W_1 = weight of portion of slice above water table

W_2 = submerged weight of portion of slice below water table

α = angle between base of slice and horizontal

h = height of slice

z = depth to base of slice below water table

γ_w = unit weight of water

For a total stress analysis, the values of cohesion (c) and angle of internal friction (ϕ), are determined by means of undrained soil tests. The trial factor of safety may also be obtained using an effective stress analysis if appropriate values are used for the parameters in Eq. (4.2).

Because the variable FS appears on both sides of Eq. (4.2) an iterative solution is needed to determine FS Convergence to a solution is rapid [31]. When using the simplified Bishop Method several potential failure surfaces must be examined The surface leading to the smallest value of FS is said to be the critical surface. The corresponding value of FS is considered to be the best estimate of the factor of safety.

4.4.2 Sources of Error- Simplified Bishop Method

The simplified Bishop method involves several sources of error. For a total stress analysis, appropriate strength parameters must be

estimated for the soil. For an effective stress analysis, the intensity and distribution of pore water pressures must be estimated along the failure surface. Terzaghi and Peck [31] indicate that generally these are the greatest source of error in estimates of stability.

A failure surface must be assumed. Generally failure is assumed to occur along a continuous circular arc. The actual failure surface may not be circular. Non-circular failure surfaces would be expected in layered embankments. Additionally, failure is assumed to take place simultaneously along the failure surface.

Equation 4.2 is based on the assumption that the forces on the vertical faces can be ignored. This assumption, which leads to the simplified Bishop method, has been reported to result in insignificant error [2,11].

Assumptions are introduced to simplify computations. The slices are assumed to be quadrilateral in shape. The weight of a slice is assumed to act vertically downward through the midpoint of the width of the slice. The base of the slice is assumed to be a plane surface.

4.5 Estimating Stability of Slopes- Finite Element Method

4.5.1 General- Finite Element Method

The finite element method is an approximate method for solving complex physical problems. This method has numerous applications. For example, the finite element method can be used to

describe the mechanical behavior of solids, heat transfer, and fluid flow. Complex geometries, excitations, and material behavior may be described. A detailed discussion of finite element analysis is provided by Reddy [24]

Using finite element analysis, one identifies a region of interest and divides the region into smaller regions called elements. Each element is assigned material properties. Boundary conditions applicable to the entire region are specified. At this point, an appropriate excitation is simulated. One can then identify a set of mathematical equations which describe the behavior of the entire region. A solution is obtained by solving these equations.

The objective in obtaining a solution for the set of finite element equations is to minimize the total potential energy functional, $\Pi(d)$. The total potential energy functional associated with the equations governing a plane elastic body is [24]

$$\Pi(d) = \frac{1}{2} h_e \int_{\Omega^e} \{\varepsilon\}_e^T \{\sigma\}_e dx\, dy - \int_{\Omega^e} \{d\}_e^T \{f\}_e\, dx\, dy - \oint_{\Gamma^e} \{d\}_e^T \{t\}_e\, ds \quad (4.3)$$

where $\{d\}_e$ = element displacement vector

$\{\varepsilon\}_e$ = element strain vector

$\{f\}_e$ = element body force vector

$\{t\}_e$ = element traction vector

h_e = thickness of element

$\{\sigma\}_e$ = element stress vector

Ω^e = element domain

Γ^e = element boundary

The following equations express the strain-displacement, the stress-strain, and the stress-equilibrium relations for the elements respectively [24].

$$\sigma_e = [D]\{u\}_e \tag{4.4}$$

$$\{\sigma\}_e = [C]_e \{\epsilon\}_e \tag{4.5}$$

$$[D]^T \{\sigma\}_e = \{f\}_e \tag{4.6}$$

where $[C]_e$ = elasticity (material) constants matrix

$[D]$ = differential operators matrix

From the above relations (Equations 4.4, 4.5, and 4.6), the element stiffness matrix is expressed as [24]

$$[K^{(e)}] = h_e \int_{\Omega^e} [B]_e^T [C]_e [B]_e \, dx \, dy \tag{4.7}$$

where $[B]_e = [D][\Psi]_e$

$[\Psi]_e$ = element interpolation functions matrix

Setting the first variation of Π with respect to the displacement vector, $\{\Delta\}$, equal to zero obtains [24]:

$$[K^{(e)}]\{\Delta^{(e)}\} = \{F^{(e)}\}$$

The element load vector resulting from the body forces is [24].

$$\{F^{(e)}\} = \int_{\Omega^e} [\Psi]_e^T \{f\}_e \, dx \, dy + \oint_{\Gamma^e} [\Psi]_e^T \{t\}_e \, ds \tag{4.8}$$

4.5.2 Modeling of Embankment Slopes- Finite Element Method

The basic considerations for finite element modeling of the slopes of earthen embankments are presented below. The

considerations include the geometry of the embankment, boundary conditions, the behavior of the embankment materials and the loading of the embankment.

The embankment being analyzed is represented as a collection of elements called a finite-element mesh. One example of a finite element mesh for an embankment slope is shown in Figure 4.3. The elements are generally triangular or quadrilateral in shape and the collection of elements has the geometry of the region of interest. The angle of the embankment slope requires special consideration when selecting the size and shape of elements located there. In such a case, specifying triangular elements in the vicinity of the slope may lead to better results.
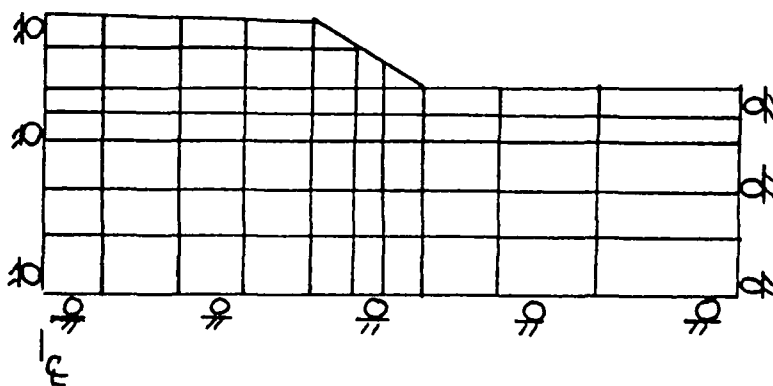

**Figure 4.3** Example of Finite Element Mesh for Embankment Slope

Boundary conditions specify behavior at the boundaries of the model. The length of an embankment perpendicular to the plane of interest is often large. In relation to the problem herein studied, the embankment modeled was 600 ft long and 250 ft wide. As a result,

plane-strain conditions are often assumed. Under plane-strain conditions deformations are not permitted perpendicular to the plane of interest. Along the base of the model roller supports were chosen. These roller supports allow free horizontal movement but do not allow vertical movement. Roller supports are also placed along both side boundaries. These supports allow free vertical movement but do not allow horizontal movement. The roller supports along the centerline allow the model to deform in a manner that would be expected of a symmetrical embankment under gravity loading. The roller supports along the other side (front) of the model allow deformations which would be expected far from the slope of the embankment under gravity type loads. The upper boundary is free. This permits unrestricted movement of the soil at this boundary.

The locations of the front side and base boundaries may be selected using Saint-Venant's principle. This would be done so that simple boundary conditions may be imposed at these boundaries. Saint-Venant's principle states that the complex stresses caused by a localized source decrease in intensity with distance from the source. Thus, Saint-Venant's principle suggests that if a simple boundary is located far enough from a source of concentrated stress, such as a finite slope, the simple boundary will closely represent correct behavior. It has been found that for models of embankment, such as that shown in Figure 4.3, the base and front side boundaries should be located at a distance of at least three times the thickness of the slope

away from the slope of the embankment [9, 24]. For the embankment herein studied, more accuracy was obtained using greater distances for the boundaries (see Appendix B).

The material properties for which values must be specified are parameters which describe stress-strain behavior. Figure 4.4 shows stress-strain curves for two types of materials. The C matrix appearing in equation 4.5 refers to the element stiffness (material elasticity) matrix which is continually updated by the stress-strain behavior of the material. The stress-strain behavior of a soil is best represented by the nonlinear curve shown in Figure 4.4(a). For computational simplicity soil is often modeled as an ideal elastic-plastic material (Figure 4.4(b)). Such a material behaves linearly to the yield stress. At this level the material may undergo unrestrained deformation.
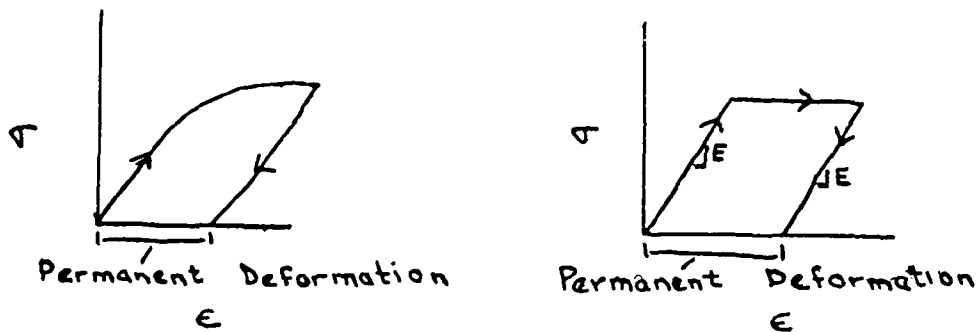
(a) Nonlinear Inelastic Material　　(b) Ideal Elastic-Plastic Material

Figure 4.4 Stress- Strain Curves

The material properties needed to define the stress-strain behavior of an ideal elastic-perfectly plastic material include the modulus of elasticity (E), a measure of the yield and Poisson's ratio (v). The modulus of elasticity relates the normal stress acting on an element of material to the resulting deformation of the element in the direction of the normal stress (Figure 4.5) [28].
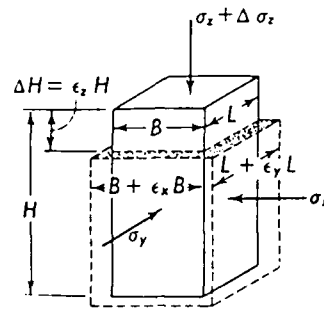
Figure 4.5 Deformation of Stressed Element

The modulus of elasticity (E) is defined as

$$E = \frac{\Delta\sigma}{\Delta\varepsilon} \qquad (4.9)$$

where $\Delta\sigma$ - increment of normal stress

$\Delta\varepsilon$ - increment of normal strain in direction of increment normal stress, $\Delta\sigma$

For an ideal elastic-plastic material, the modulus of elasticity is the slope of the linear portion of the stress-strain curve (Figure 4.4(b)).

A material that does not show permanent deformation on unloading is called an elastic material. A material which does show permanent deformation on unloading is called an inelastic (or plastic) material (Figure 4.4). Soils are generally inelastic materials but, may be assumed to behave elastically up to a certain level of stress. Generally, the region on the stress-strain curve for which there is a large increase in strain with only a small increase in stress is the

plastic region (Figure 4.4). Generally, a material is said to have failed plastically if stresses are in this region.

The strength of greatest interest for stability estimates is the shear strength of a soil (s). The shear strength is usually determined by triaxial tests. In such tests axial and radial normal stresses are applied to a cylindrical sample of soil. Generally, the radial stress is held constant while the axial stress is increased until the sample fails. Typically, unconsolidated-undrained triaxial tests are performed on clayey soil samples to provide information needed for total stress analyses [28].

For finite element modeling a failure criteria must be specified for each element. One can establish an appropriate failure criterion for an element of soil based on a suitable available failure criterion and the results from triaxial tests. The von Mises or Tresca failure criterion are generally considered to be suitable for metals and alloys. As the shear strength of the soil depends on the confining pressure, the Mohr-Coulomb failure criteria will best represent the failure of soils. However, for simplicity, the von Mises criterion is chosen here. The von Mises failure criterion is expressed as

$$2 \sigma_f^2 = (\sigma_x - \sigma_y)^2 + (\sigma_y - \sigma_z)^2 + (\sigma_z - \sigma_x)^2 \qquad (4.10)$$

where σ_f = von Mises failure stress of material

$\sigma_{x,y,z}$ = principal stresses in x, y and z directions, respectively

An element is said to have failed when the combination of principal stresses acting on the element is such that the right side of Equation 4.10 equals or exceeds the left side. The quantity σ_f may be specified for an element based on triaxial test results. Test values of σ_x, σ_y and σ_z at failure are substituted into Equation 4.10. For an unconsolidated-undrained triaxial test σ_x and σ_y are both equal in value to the radial stress. The quantity σ_z is equal in value to the axial stress. Equation 4.10 is solved for σ_f and the value obtained is specified the von Mises failure stress of the element of interest.

Poisson's ratio relates vertical and horizontal deformations of an element of material under load. When an axial (vertical) compressive load is applied to an element of material the element will expand laterally (horizontally) (Figure 4.5). Poisson's ratio is defined as the negative of the ratio of the lateral normal strain (ε_x or ε_y) to the axial normal strain (ε_z).

$$\upsilon = \frac{-\varepsilon_x}{\varepsilon_z} = \frac{-\varepsilon_y}{\varepsilon_z} \qquad (4.11)$$

Poisson's ratio for soils usually ranges from 0 to 0.5 [28]. A Poisson's ratio of 0.5 indicates that there would be no volume change upon loading.

A material may be isotropic or anisotropic and a mass of material may be homogeneous or nonhomogeneous. An isotropic material has the same mechanical properties (i.e., E and υ) in all directions. A homogeneous mass of material has uniform properties

throughout. Most naturally occurring soils are anisotropic and most soil deposits are nonhomogeneous. However, soil deposits or layers are often modeled as isotropic and homogeneous for convenience.

The loads for a model of an embankment may include the weights of the various soil layers and water, and surcharges. One can account for the effects of a horizontal water table in several ways. For example, for a total stress analysis the hydrostatic water pressure acting on a submerged surface may be represented as a distributed load applied to the surface of appropriate elements. The water below the water table and within the soil can be accounted for by using the saturated unit weight (γ_{sat}) of the soil.

To carry out a finite element analysis for an embankment, the material properties, boundary conditions, and loads associated with each element are specified. Element stiffness matrices and force and displacement vectors are formed.

Based on equilibrium at each node, a set of simultaneous equations is developed. A solution is obtained by solving this matrix equation for unknown nodal displacements. The matrix equation involves a global stiffness matrix and a load vector, which are formed by combining the corresponding element quantities. Stresses and strains for elements are derived from the solution. This procedure describes the steps needed to obtain a linear elastic solution.

An iterative solution procedure is required if an elastic-plastic model is used. In such a case the embankment load is applied incrementally. The stiffness matrix is updated iteratively within each

increment of loading to account for the nonlinear behavior. The
iterations are terminated when a preset tolerance criterion for nodal
[illegible] be satis[illegible]. The nonconvergent state is generally taken
to represent a global failure of the structure.

The factor of safety for the slope of an embankment may be
defined as the fraction of the gravity load applied which causes
failure. Failure may be said to occur at the level of gravity load for
which either a nonconvergent solution is obtained or a continuous (or
near continuous) band of yielded elements exists across the slope of
the model. A yielded element may be identified as an element for
which the specified von Mises stress is obtained at integration points.

The estimated factor of safety based on finite element analyses
is normally specified as a continuous band of yielded elements. This
failure criterion is related to a continuous potential failure arc as
specified by the simplified Bishop method. The factor of safety in
both methods is based on the shear stress exceeding the shear
strength along a specified surface.

For finite element analysis, the geotextile layer can be
represented by additional elements within the embankment model.
Material properties, boundary conditions, and location of the elements
are specified which best represent the geotextile layer.

4.5.3 Sources of Error- Finite Element Method

The finite element method as applied to estimating the stability
of embankment slopes generally involves several sources of error or

uncertainty. For geotechnical analyses the values used for soil properties may have a significant effect on results from the analyses. It is believed, in general, that soil properties must be determined to a reasonable level of accuracy and in reasonable detail for the effective use of finite element analysis.

The failure criterion used for a finite element analysis may also create uncertainty. A specified failure criterion may not apply to all types of loading.

The loading sequence may have an effect on the results obtained using the finite element method. Loading sequences which model actual construction sequences may provide the best results.

Chapter 5

Stability Analyses for Embankment Slope at Washington National Airport

5.1 Introduction

In this chapter the stability of the slope of the East-West side of the safety overrun of Runway 18 at Washington National Airport is investigated. Analysis results obtained by the U.S. Army Corps of Engineers using the simplified Bishop method (see Chapter 4) are summarized. Analysis results obtained at The Johns Hopkins University using the finite element method (see Chapter 4) are presented and discussed. The results obtained using the two methods are compared.

5.2 Stability Analyses - Simplified Bishop Method

Stability analyses were performed for the embankment of interest by the Baltimore District Corps of Engineers using a computer program entitled Slip Circle Slope Stability with Side Forces (computer program 741-11-F5030) [27]. This program, developed by the Corps of Engineers, is based on the simplified Bishop method of analyzing the stability of slopes.

Conditions judged to be critical for design are shown in Figure 5.1. Based on results from their analyses, the Corps of Engineers

concluded that the East-West slopes of the runway embankment were the least stable and that the end-of-construction conditions would be critical for design purposes. These conclusions were based on assuming minimum values for soil strengths. The results from analyses conducted by the Corps of Engineers for the East-West sides of the runway overrun assuming end-of-construction conditions and minimum values for soil strengths are discussed below. Results are discussed from analyses which considered an unreinforced embankment and an embankment reinforced with a geotextile.

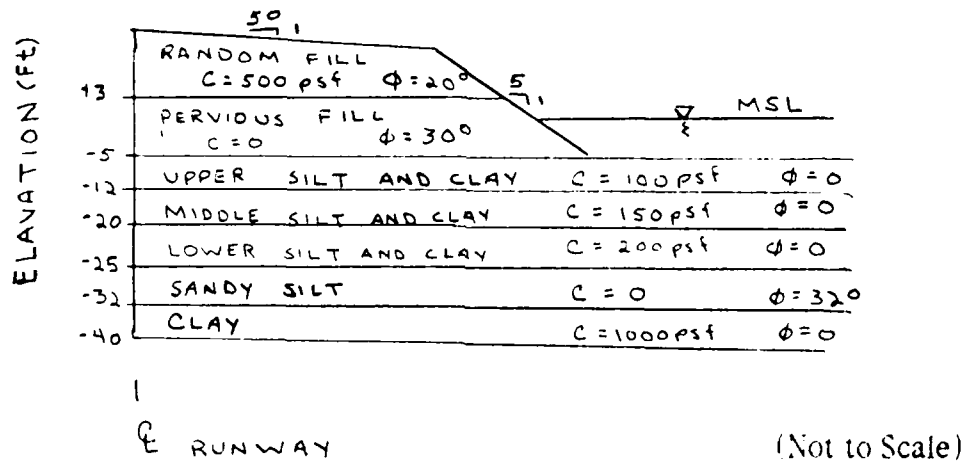**Figure 5.1** Critical Conditions for Design

5.2.1 Unreinforced Embankment

The soil data used for the analyses of the East-West slopes of the embankment of interest are shown in Table 5.1 [27]. This table, and Figure 5.1 are based on the assumption of construction on the existing foundation soil. The random and pervious granular fills were assumed to add a weight load on the existing foundation soil.

However, it was assumed that tension cracks may develop in these layers. Thus, these layers were not considered to provide resistance against a slope failure in the slope stability analyses.

The critical potential failure surface is shown in Figure 5.2 [27]. The corresponding factor of safety was calculated to be 0.81. This was less than the required factor of safety of 1.2 for end-of-construction conditions and indicated that the soft foundation soil could not support the embankment.

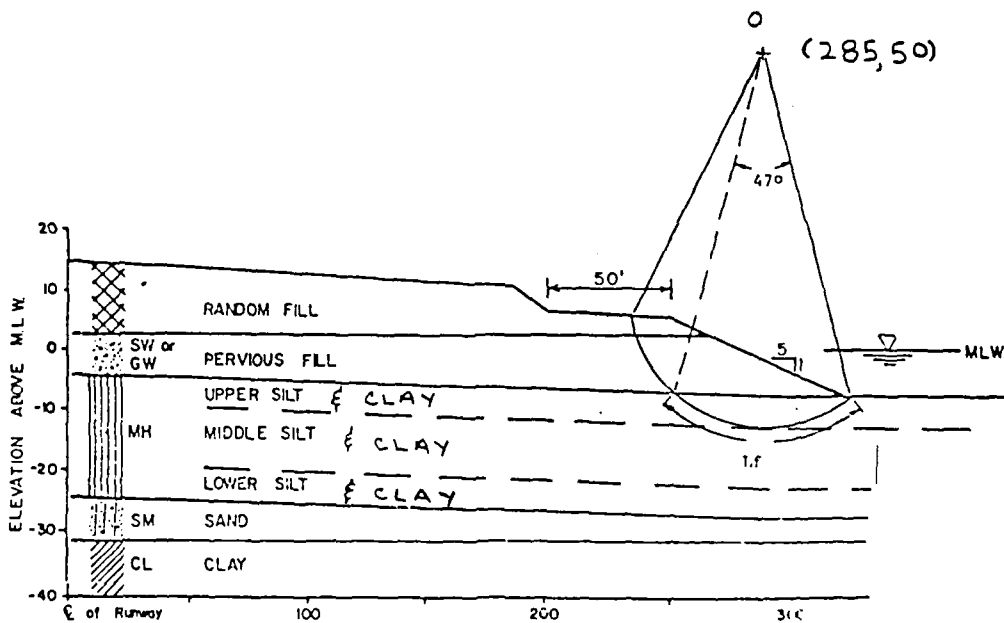| Soil Type	γ_{sat} (pcf)	Shear Strength U-U (Q) Min	
		ϕ	c (psf)
Random Fill	125	20	500
Pervious Fill	115	30	0
Upper Silt	90	0	50
Middle Silt	90	0	150
Lower Silt	90	0	200
Sandy Silt	120	32	0
Clay	115	0	1000

Table 5.1 Summary of Soil Data

Figure 5.2 Critical Potential Failure Surface-
Unreinforced Embankment

5.2.2 Embankment Reinforced with Geotextile

The model discussed above was modified to include the additional resistance provided by a reinforcing geotextile. The Corps of Engineers have developed a method for estimating the tensile sterngth (T_f) required of a reinforcing geotextile for a desired level of slope stability [6]. The method is based on the simplified Bishop method of analysis (see Chapter 4) and involves two steps.

First, a rough estimate is made of the tensile strength needed from the reinforcing geotextile for a desired factor of safety against a slope failure. For this a critical arc is established for the appropriate unreinforced slope using the simplified Bishop method. The depth ratio (D) (see Figure 5.3) is calculated.
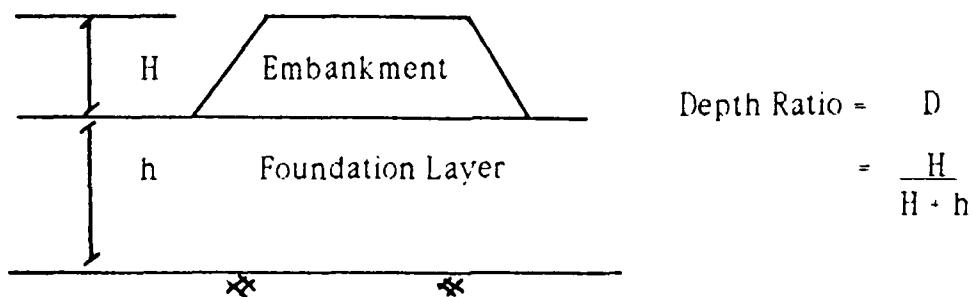

Figure 5.3 Depth Ratio

A total stability number for the embankment, N, is obtained for a specified factor of safety from a design curve (see Appendix A, Figure A.2). A stability number for the foundation layer, N_u, where N_u =

c/(γH), is calculated. A stability number for the geotextile, N_f, is calculated as

$$N_f - N - N_u \qquad (5.1)$$

The equivalent cohesion required of the geotextile, c_f, for the specified factor of safety is calculated as

$$c_f - N_f \cdot \gamma_h \cdot H \qquad (5.2)$$

where γ_h - unit weight of embankment.

A second design chart (see Appendix A, Figure A.3) is used to estimate the required geotextile strength, (T_f), from the depth ratio and equivalent cohesion, c_f. Appendix A contains a flowchart for the above procedure.

Second, a more rigorous stability analysis is conducted to determine more precisely the factor of safety of the reinforced slope. The geotextile is considered to provide additional cohesion, based on the strength estimated for the geotextile as described above, to layers which provide shear resistance (see Figure 5.4) [6].
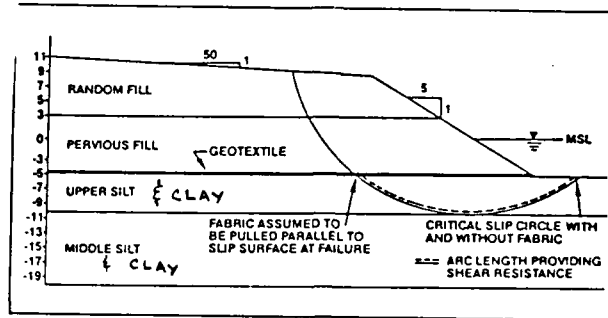
Figure 5.4 Critical Potential Failure Surface- Geotextile
Reinforced Embankment

The equivalent cohesive strength provided by the geotextile (c_f) is
expressed as:

$$c_f = \frac{T_f}{L_f} \tag{5.3}$$

where L_f = length of the failure arc in soil layer in foundation soil
beneath geotextile

Failure is assumed to occur along the potential failure arc indicated by
the simplified Bishop method for the corresponding unreinforced
embankment (see Figure 5.2).

Basically with this method, it is assumed that the tensile
strength of the geotextile and the shear strength of the soil are
mobilized simultaneously.   Additionally, with this method it is

assumed that the tensile strength provided by the geotextile is directed tangent to the potential failure arc at failure.

The properties of the geotextile in the warp (lengthwise thread) direction were judged to be critical for the stability analyses [19]. The tensile force at failure was taken to be the tensile force corresponding to an elongation of 5%. This tensile force was specified as 200 lb/in.

Summarizing the results obtained by the Corps of Engineers, from their stability analysis for the reinforced embankment the critical potential failure surface was, by assumption, identical to that estimated for the unreinforced slope (see Figure 5.2 and 5.4). The equivalent cohesion of the geotextile was calculated to be 47.2 psf and the factor of safety of the slope, based on minimum shear strength, was estimated to be 0.99.

Though the factor of safety obtained was less than the required factor of safety (1.2), based on average shear strength, the Corps of Engineers was willing to accept the lower factor of safety in the very few isolated locations where the soil strength was judged to have the minimum value.

5.3 Stability Analyses- Finite Element Method

The finite element stability computations were performed using the commercial program 'BAQUS' production version 4.5 171 dated July 1992. The program was developed by Hibbit, Karlsson and Sorensen, Inc., Providence, R.I. Results obtained modeling both unreinforced and reinforced embankments are presented below. A detailed description of the model development is provided in Appendix B.

5.3.1 Unreinforced Embankment

The unreinforced embankment corresponding to the model developed by the Corps of Engineers and shown in Figure 5.2 was modeled using the finite element method. For each model, as indicated by the model shown in Figure 5.5, symmetry was assumed about the centerline of the embankment. The mesh consisted of 455 quadrilateral elements. Each element was a four node rectangle, type CPE4H selected from the ABAQUS element library for plane strain conditions. The mesh was formed such that element boundaries coincided with the boundaries of the soil layers. This simplified specification of material properties.

Saint-Venant's principle (see Section 4.5.2) was used to locate the base and right side boundaries. The base boundary was placed 59 ft. below the mean level of the water. The right side of the model was located 560 ft. from the centerline. Thus, the base boundary was 4 times the height of the slope from the slope, and the right side
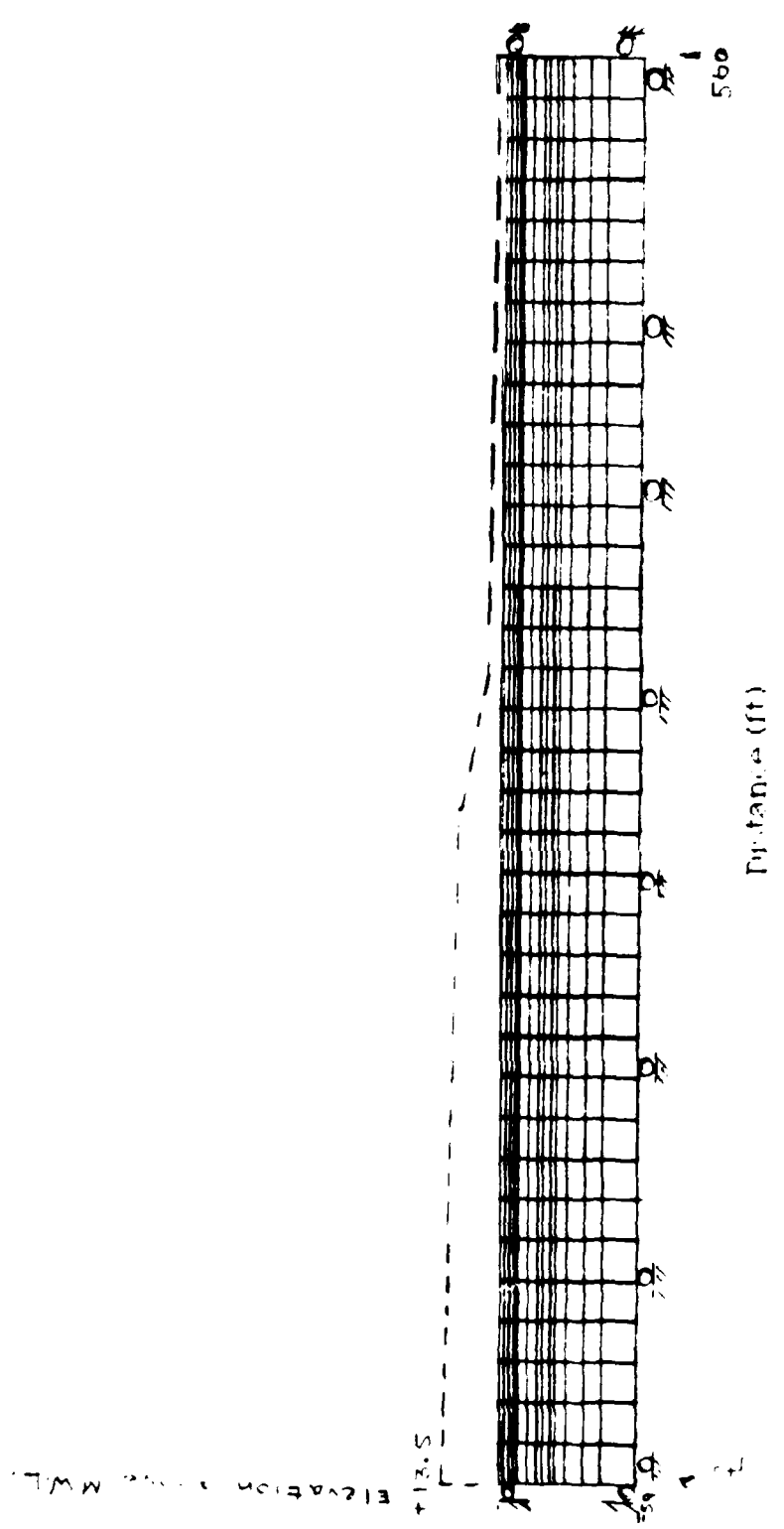
Figure 55 Mesh for Finite Element Analysis – Unreinforced Embankment

boundary was 18 times the thickness of the slope from the slope. These boundaries were established from preliminary convergence studies (see Appendix B).

Values for the soil properties used for the finite element analyses are given in Table 5.2.

Soil Type	E_s (ksf)	υ	c (psf)	ϕ (deg.)	σ_f (psf)	K_0	γ_{sat} (pcf)
Random Fill	0	0	0	0	0	0	125
Pervious Fill	0	0	0	0	0	0	115
Upper Silt & Clay	100	0.50	50	0	100	0.6	90
Middle Silt & Clay	200	0.50	150	0	300	0.6	90
Lower Silt & Clay	250	0.50	200	0	400	0.6	90
Sandy Silt	364	0.35	0	32	6116	0.6	120
Clay	1000	0.50	1000	0	2000	0.6	115

Table 5.2 Soil Properties Used for FEM Analyses

The work described herein was carried out assuming the soil within each layer to be isotropic. homogeneous and to behave as a linearly elastic-plastic material. Because of the assumption of tension cracking. the strengths of the upper two layers were neglected. Values for the elastic parameters, E_s and υ, were selected from typical ranges provided by Bowles [3]. The effective coefficients of earth pressure at rest, K_0, were selected from typical values provided by Sowers [28] As discussed in the paragraph below. the failure stresses for the soil layers were derived from the unconsolidated-undrained strength parameters. c and ϕ, estimated by the Corps of Engineers [27]. Soil

layers located beneath the clay layer were given the properties of the clay layer.

The von Mises stresses, σ_f, for the foundation soils were obtained using the unconsolidated-undrained strength parameters, c and ϕ, based on results from triaxial tests. For the silt and clay soils (ϕ = 0), the radial confining stress, and thus, σ_x and σ_y, was taken to be equal to zero. From Equation 4.5, the von Mises failure stress becomes

$$\sigma_f = \sigma_z \tag{5.4}$$

where σ_z = axial normal stress at failure.

Since the axial stress at failure, in an unconsolidated-undrained triaxial test conducted on a soil sample for which $\phi=0$, is larger than the radial confining stress by the amount 2c for clay and silt soils, the failure stress was specified as

$$\sigma_f = 2c \tag{5.5}$$

To estimate the von Mises failure stress for the sandy silt layer it was first necessary to estimate the average lateral stress within the layer. This was necessary so that the strength of the soil under unconsolidated-undrained conditions in a triaxial test could be estimated. The average lateral stress, σ_h, was obtained from the static total overburden pressure at the center of the sandy silt layer using the following equation [28]:

$$\sigma_h = (\Sigma \gamma h + \Sigma \gamma' h) K'_0 + \gamma_w z \qquad (5.6)$$

where γ = total unit weight of soil layer above the water table
γ' = effective unit weight of soil layer below water table
K'_0 = effective coefficient of earth pressure at rest
γ_w = unit weight of water
h = thickness of layer (1/2 thickness for sandy silt layer)
z = depth of water (to center of sandy silt layer).

A radial confining pressure equal in value to σ_h was assumed to be applied to a triaxial test sample from the sandy silt layer. The axial stress acting on the sample at failure, was estimated using the following equation based on the Mohr-Coulomb failure criterion:

$$\sigma_z = \sigma_h \cdot \tan^2(45^0 + \phi/2) + 2c \cdot \tan(45^0 + \phi/2) \qquad (5.7)$$

where ϕ = angle of internal friction for unconsolidated-undrained conditions

Substituting $\sigma_x = \sigma_y = \sigma_h$ into equation 4.10, the von Mises failure stress was obtained as

$$\sigma_f = \sigma_z - \sigma_h \qquad (5.8)$$

The loading of the model required special attention. Using the ABAQUS program, we were not able to specify a value of zero for the von Mises failure stress (see Appendix B). It was necessary to model

the random fill and pervious fill layers as a vertical surcharge acting along the surface of the foundation soils (see Figure 5.5). This surcharge was added to that corresponding to the water surrounding the embankment. The loading due to the weight of the foundation soil was treated as a gravity loading.

The loads from the embankment, its foundation, and the water surrounding the embankment were applied simultaneously in increments. The incrementing of load was initiated at 20% of the full gravity load and increased at minimum increments of 0.5%. The tolerance for a convergent force solution was specified as 10 lbs. Thus, a convergent solution was said to have been obtained if each of the element load values at the nodal integration points from an iteration were within 10 lbs. of those obtained from the preceding iteration.

The factor of safety for the slope of the unreinforced embankment was estimated to be 1.00 based on the development of a nearly continuous band of yielded elements across the slope. Figure 5.6 shows the band of elements which yielded under the load corresponding to failure. A mesh showing the deformation of the embankment under this load is presented in Figure 5.7 along with an outline of the original undeformed mesh.

47

Failure Circle - Simplified Bishop Method

NODE 17
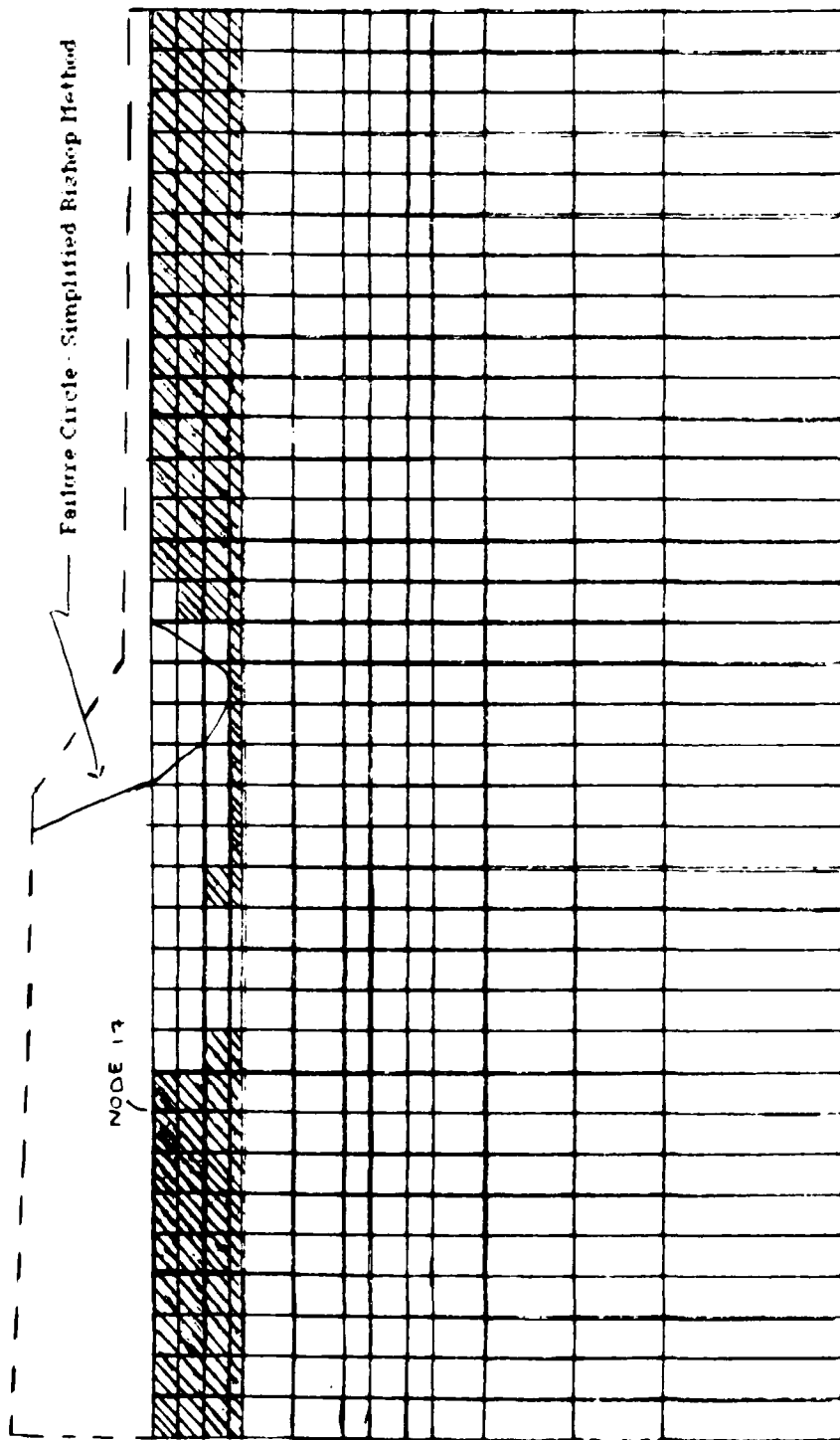
Yielded Element

Height exaggerated by a factor of 5

Figure 5 6 Mesh Showing Yielded Elements in Upper Silt & Clay Layer at Failure Load -
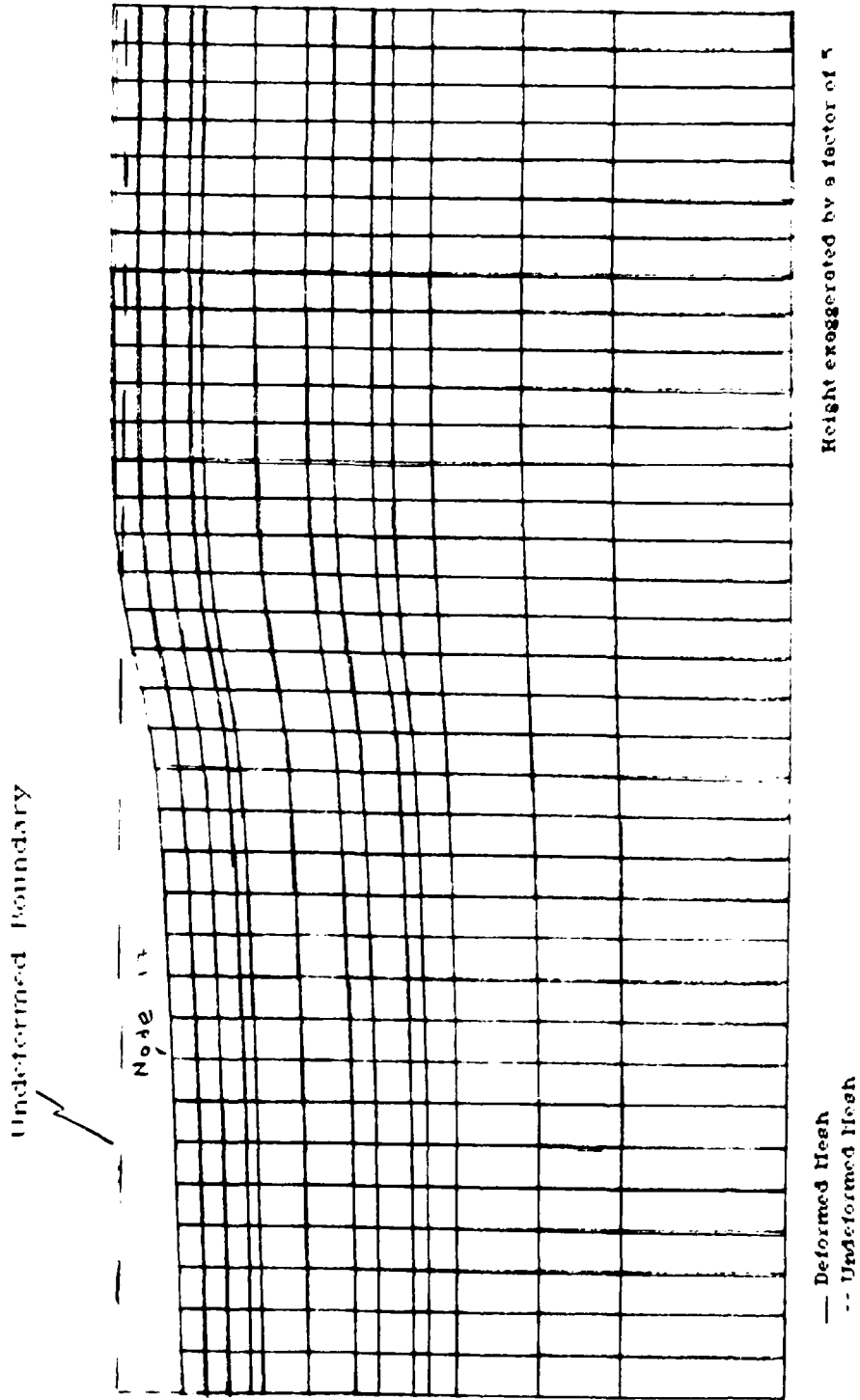Unreinforced Embankment Slope (FS = 1 0)

Figure 5.7   Deformed Mesh at Failure Load — Unreinforced Embankment Slope (FS = 1.0)

5.3.2 Embankment Reinforced with Geotextile

The reinforced embankment corresponding to the model developed by the Corps of Engineers was modeled using the finite element method. Basically, elements representing a single geotextile layer reinforcing the embankment were added to the model of the unreinforced embankment discussed in section 5.3.1.

The geotextile was represented as a thin one dimensional layer placed on top of the upper silt layer. The elements representing the geotextile layer were allowed to withstand tension forces only. The element selected from the ABAQUS element library to represent the geotextile was a two node element, type C1D2. The geotextile layer was specified to extend from the centerline of the model to a distance of 50 feet beyond the edge of the embankment slope. The thickness of this additional layer was specified to be 0.100 in.

It was specified that no slip could occur between the geotextile elements and the soil elements. This was done to model the geotextile following the deformation of the upper layer of the soil. The boundary of the geotextile layer at the centerline of the model was represented as a vertical roller. The boundary at the other end of the geotextile layer was specified as free.

The properties of the geotextile layer used for the finite element analysis were based on the material properties specified by the manufacturer. The properties specified for the finite element analysis are shown in Table 5.3. The failure stress of the geotextile, σ_f,

was obtained by dividing the tensile force at 5% strain within a specified portion of the geotextile by the cross sectional area of the geotextile. The modulus of elasticity was obtained by dividing σ_f by this strain.

Modulus of Elasticity, E_s	5760 ksf
Poisson's Ratio, υ	0.3
Failure Stress, σ_f	288000 psf

Table 5.3 Properties of Geotextile Layer Specified for Finite
Element Analysis

The same loads that were applied in the case of the unreinforced embankment (see Section 5.3.1) were applied in the case of the reinforced embankment. The weight of the geotextile layer was considered insignificant. To determine the factor of safety and failure surface the loads were applied to the elements representing the geotextile layer and to the elements representing the foundation soil. The applied loads were transfered to the nodes joining the elements that represented the geotextile layer were specified to be common to the upper nodes of the elements representing the upper silt layer.

The factor of safety for the slope of the reinforced embankment was estimated to be 1.00 based on the development of a nearly continuous band of yielded elements across the slope. Figure 5.8 shows the band of elements which yielded under the load corresponding to failure. A mesh showing the deformation of the
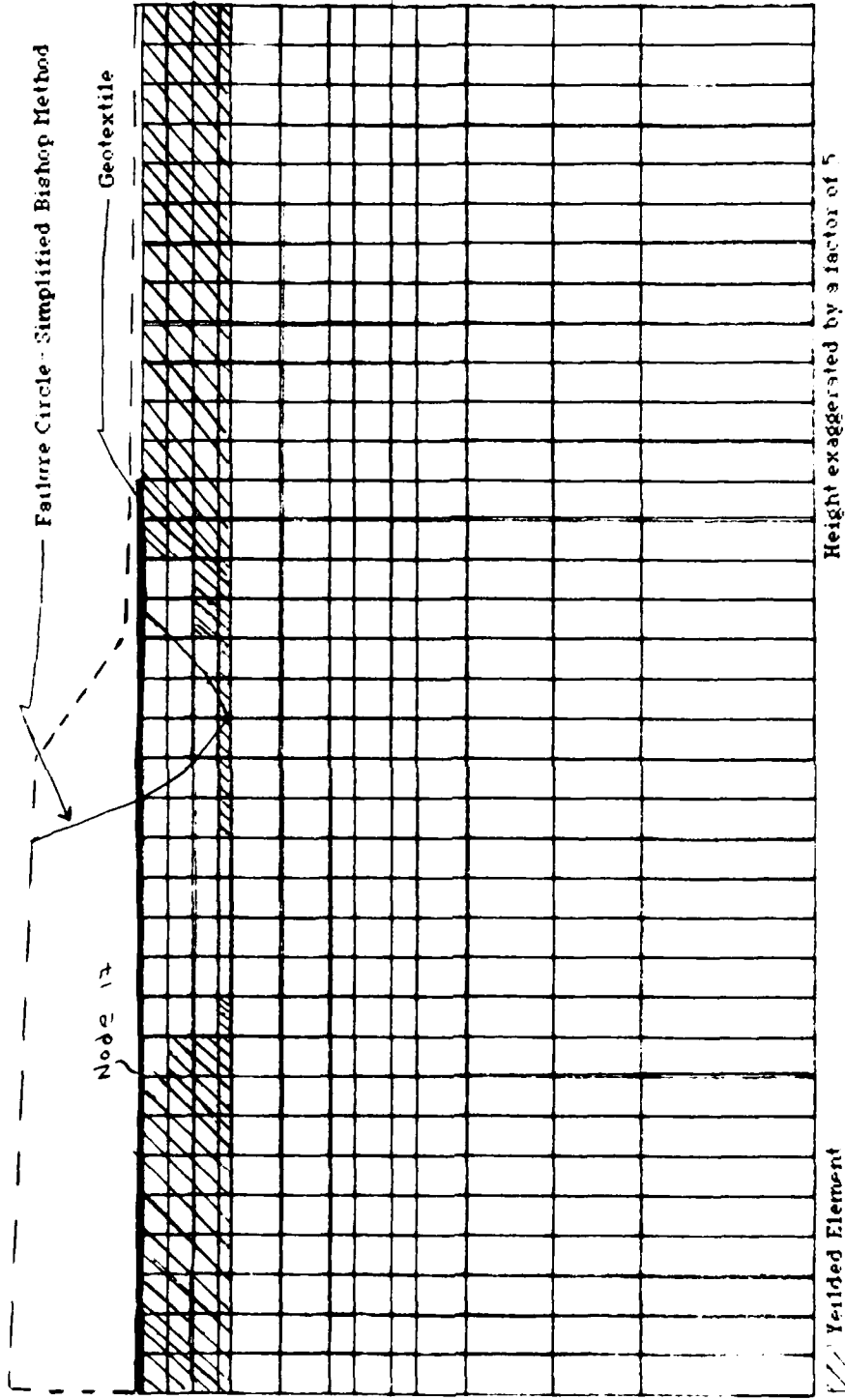
Figure 5.8 Mesh Showing Yielded Elements in Upper Silt & Clay Layer at Failure Load- Reinforced Embankment Slope (FS = 1.0)
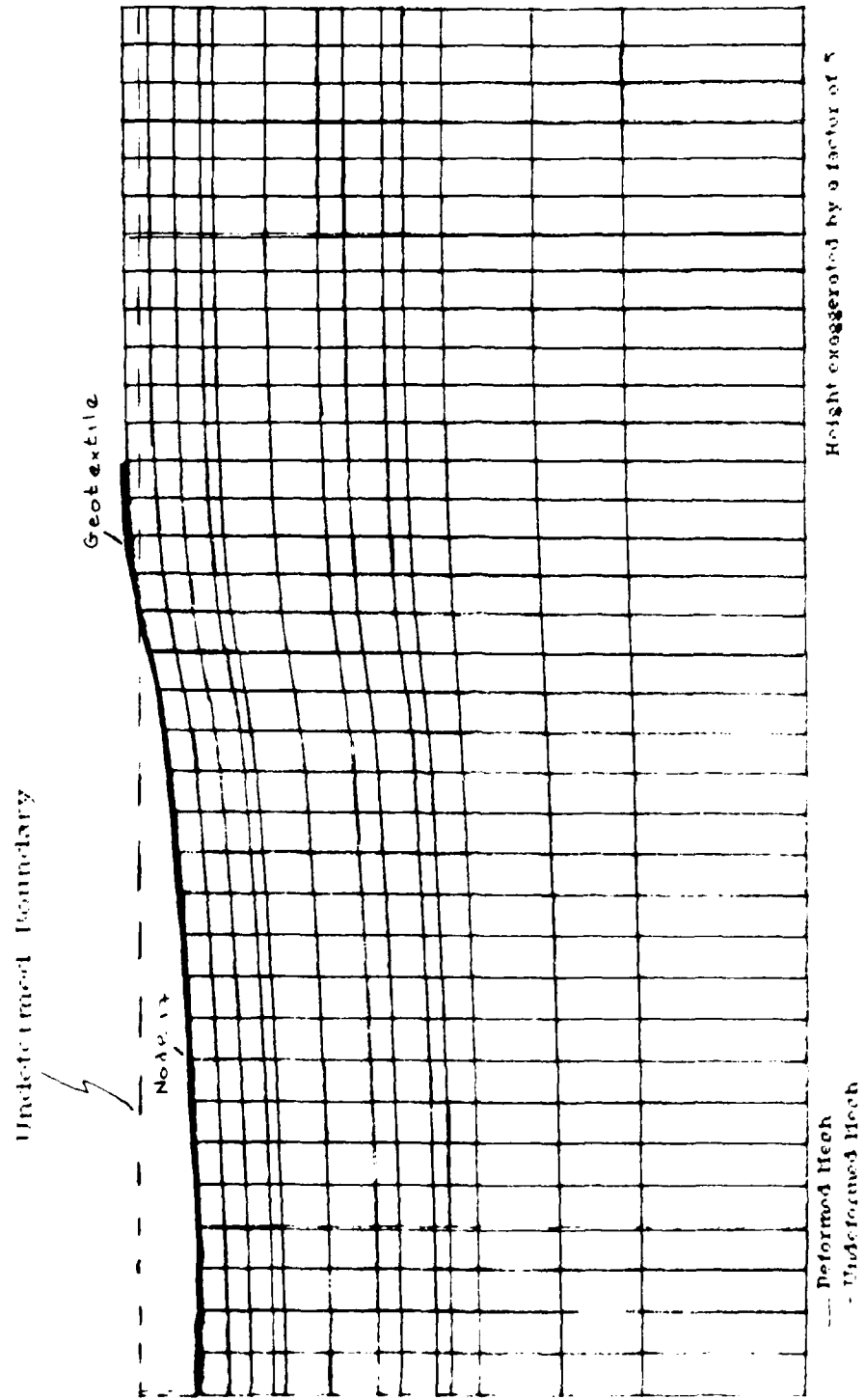
Figure 5.9   Deformed Mesh at Failure Load - Reinforced
Embankment Slope (FS = 1.0)

embankment under this load is presented in Figure 5.9 along with an outline of the original undeformed mesh.

5.4 Discussion of Result: Finite Element Method

Results obtained by the Corps of Engineers using the simplified bishop method are compared to results obtained at The Johns Hopkins University using the finite element method. The comparisons as well as the results obtained using the finite element method are discussed. Possible sources of error in the results obtained using the finite element method are presented.

5.4.1 Discussion and Comparison of Results- Finite Element Method

The factors of safety estimated using both the simplified Bishop method and finite element method are presented together in Table 5.4. Reasonably close agreement was observed between the factors of safety obtained using the two methods. The factors of safety estimated using the finite element method were higher than the corresponding factors of safety estimated using the simplified Bishop method. As would be expected the modeling of a reinforcing geotextile resulted in an increase in the factor of safety obtained by each method. However, the increase observed using the finite element method was much less than that observed using the simplified Bishop method.

	Factor of Safety	
	w/o Geotextile	w/ Geotextile
Simplified Bishop Method	0.81	0.99
Finite Element Method	1.00	1.00
Percent Difference	19%	1%

**Table 5.4** Estimated Factors of Safety

There was difficulty in obtaining nonconvergent solutions using the finite element method. Nonconvergence was not observed in any of the solutions presented herein, even at levels of loading that corresponded to twice those due to gravity. These difficulties were understood to result from the use of linear elastic-plastic material modeling. Apparently, this type of modeling creates conditions under which it is fairly difficult to obtain nonconvergent solutions.

The factors of safety obtained for the two models of the embankment slope using the finite element method were to be based on studying both the yielded elements and embankment displacements as functions of the fraction of gravity load applied. A factor of safety based on yielding was defined as the fraction of the full gravity load for which a continuous or nearly continuous band of yielded elements was observed to develop across the slope of the embankment (see Figure 5.10 (a) & (c)). An element was arbitrarily considered to be yielding when the stresses at each integration point were such that the right side of equation 4.10 was equal to or greater

than 98% of the left side. A factor of safety based on displacements was defined as the fraction of the full gravity load for which a distinct change in the rate of change of the total vertical displacements was observed for the embankment slope (Figure 5.10 (b) & (d)).

The final estimates of the factors of safety were based on the fractions of gravity load for which the greatest number of yielded elements appeared across the face of the slopes. This method was selected because, for the given set of results, it was easier to physically relate failures to the number of yielded elements across the slope than to the vertical displacements of the slopes.

As indicated in Figures 5.6 and 5.8, fair agreement was obtained between the failure surfaces predicted by the simplified Bishop method and the finite element method. The failure surfaces predicted by the finite element method are the surfaces which separate the nearly continuous bands of yielded elements across the slopes from the nonyielded elements above. These surfaces agree roughly with the corresponding circular failure surfaces predicted using the bishop method. As would be expected, in each case the failure surface passes through the weakest layer of soil. It was found that the progressive development of failure surfaces may be studied using the finite element method by examining the behavior of finite element meshes under different levels of load. Basically, under loads of low enough level no elements yield. Then as the load is increased more elements yield. With a large enough load one may observe failure
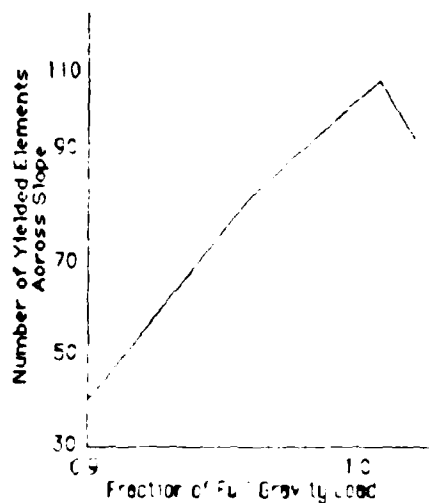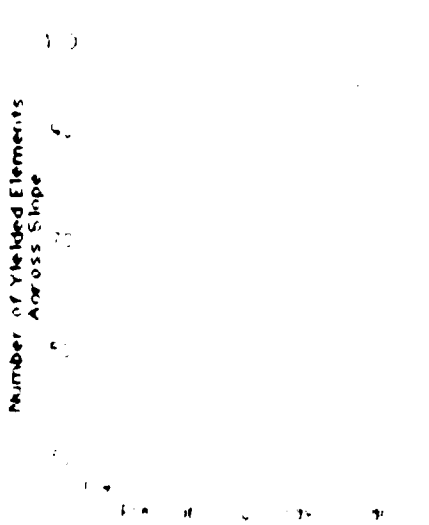
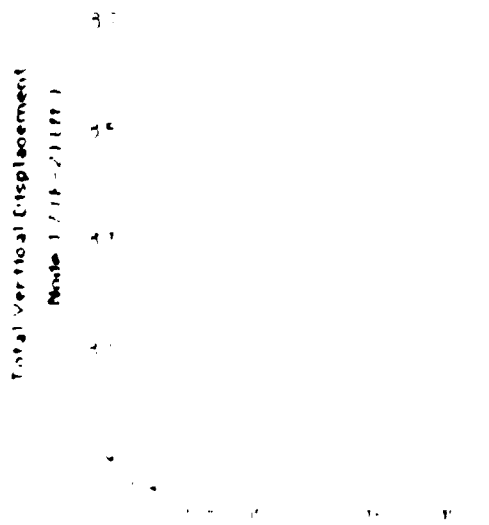(a) No. of Yielded Elements
vs Load
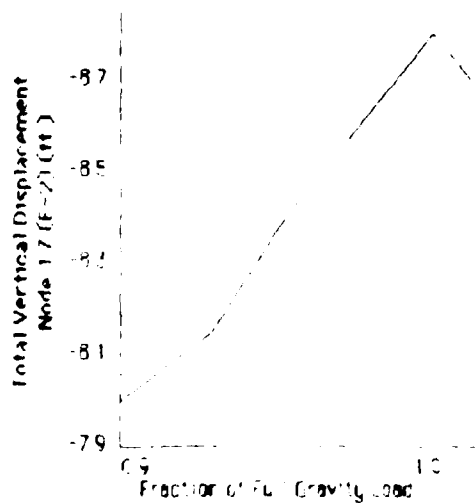
(b) Total Vertical Displacement
Node 17 vs Load

UNREINFORCED MODEL

(a) No. of Yielded Elements
vs Load

(b) Total Vertical Displacement
Node 17 vs Load

REINFORCED MODEL

Figure 5 10

The apparent lack of distinct sliding masses makes it difficult to
[illegible] The finite element method
predicted that the upper regions of the slopes would drop while the
lower region would rise However, distinct sliding masses which had
slipped relative to the surrounding regions were not observed. It was
found that the progressive development of deformations may be
studied using the finite element method by examining the behavior of
finite element meshes under different levels of load

5.4.2 Sources of Error Finite Element Method

This section discusses the major sources of uncertainty in the
results obtained using the finite element method. This discussion
differs from that of Section 4.5.3 in that the discussion in Section 4.5.3
was general whereas the discussion in this section relates to the
author's experience gained during the course of this study.

One source of error or uncertainty in the estimates of the
factors of safety for the embankment slopes is the imprecision
involved with defining the failure load. Neither the method of
defining the failure load based on yielded elements nor the method
based on slope displacement was found fully satisfactory

There is no particular or the one unique way of defining the
failure load point. It is difficult to compare the factor of safety
calculated by the finite element method with the factor of safety

calculated by the simplified Bishop method unless a common basis can be identified.

Another source of uncertainty was the description of soil behavior. Failure criteria were specified as independent of states of stress. However, failure in a soil would be expected to depend on the state of stress. The failure criteria used for the soil layers of the finite element models were based on results from triaxial compression tests. The triaxial compression test involves a state of stress which is *relatively simple compared to the states of stress experienced by soil* elements during the finite element analyses.

The manner in which the finite element models were loaded involved uncertainty. All loads were applied simultaneously. A more realistic loading sequence would have been one which simulated more closely the actual deposition/construction sequence.

In developing the finite element models it was assumed that the upper two layers do not contribute to shearing resistance. These layers were modeled as a distributed vertical load. However, these *layers do have the strength to maintain internal stability and would* be expected to provide at least some resistance to a failure of the slope.

An effective stress analysis may have resulted in somewhat more accurate predictions of the behavior of the embankment slopes than a total stress analysis. Treating the soil structure and water separately, as is done in an effective stress analysis, allows each of

these components to be assigned property values which better represent material behavior under load.

Chapter 6

Summary, Conclusions and Future Work

6.1 Introduction

In this chapter a brief summary of the work described herein is presented and conclusions are provided. Future work is also suggested.

6.2 Summary of Work

An existing, partially submerged embankment constructed on a layered soil deposit was analyzed using the finite element method. This was done to study the applicability of the finite element method to the design of the slopes of embankments. Only loads due to gravity were considered to act on the embankment. Analyses were conducted for the embankment both with and without a reinforcing geotextile. Factors of safety were estimated for slopes of the embankment from the results of the analyses. These factors of safety were compared with factors of safety estimated for the slopes by the Baltimore District of the U.S. Army Corps of Engineers. The Corps of Engineers who had designed the embankments, used the simplified Bishop method for their estimates. Also, the development of overall failure of the slopes of the embankment as described by the finite element

analyses and the deformed shapes of the embankment at failure were studied.

6.3 Conclusions

The finite element method appears capable of providing detailed, physically reasonable descriptions of the behavior of embankment slopes. Fair agreement was observed between the factor of safety obtained using the simplified Bishop method and those obtained using the finite element method. The finite element method resulted in higher factors of safety. The modeling of a geotextile resulted in increased factors of safety however, the results of the finite element method were found to be relatively insensitive to the presence of a reinforcing geotextile. The finite element solutions for the unreinforced and reinforced embankment had the same estimated factor of safety (1 0) and the same failure surface

The finite element method may be useful for describing the progressive development of the failure of slopes of embankments. For this the behavior of an embankment would be examined under different levels of load. Initially under low levels of loading elements would not be expected to yield. However, as the load is increased yielding of elements would be expected. At a large enough load a continuous or reasonably continuous band of yielded elements would be expected to develop across the slope indicating failure of the slope

More simply perhaps the development of the deformations of the embankment under load may be studied using the finite element

method. However, the finite element method, as used in the study described herein, does not appear to describe a failure mass which has distinctly slipped relative to its surroundings.

Some difficulties were encountered in the use of the finite element method. It was found to be difficult to precisely define a state of failure. The most reasonable method for defining a state of failure seems to be a method based on the number and distribution of yielded elements. Also, the modeling of a soil mass having either little shear or little tension strength was found to be difficult.

The finite element method appears to be a potentially effective method for providing refined estimates of the behavior of the slopes of embankments. This method appears to have the capability of reasonably closely modeling the progressive nature of slope failures, complex geometries, complex stress-strain behavior, and complex loadings as well as soil layering, submergence beneath water, and reinforcement from a geotextile. However, considerable effort and specialized experience may be needed to effectively conduct finite element analyses. Additionally, costly specialized soil testing may be needed to determine soil properties to the level of accuracy and in the detail believed to be necessary for the effective use of the finite element method. As a result of the features and drawbacks of the finite element method, it is felt that this method would be most appropriate for the advanced stages of the design of critical facilities.

6.4 Future Work

There are several areas toward which future work should be directed. The future work would be intended to advance the ability of the finite element method to describe the behavior of embankment slopes.

Work should be directed at developing a method for precisely defining the state of failure and subsequently a definition for the factor of safety. There is no unique way of defining the factor of safety, and this is particularly true when one attempts to compute a factor of safety from finite element results. It is difficult to compare the factor of safety calculated by the finite element method with the factor of safety calculated by the simplified Bishop method, unless a common basis can be identified.

In the future attention should be directed at the modeling of soil which has either little shear or little tensile strength. Other areas toward which attention should be directed include the modeling actual of loading sequences, use of effective stress analyses, accounting for partial dissipation of excess pore water pressures and the development of boundary conditions which can describe more effectively the behavior of regions surrounding the region of interest.

Appendix A
Geotextile Design Charts

A.1 Introduction

In this appendix geotextile design charts developed by the Corps of Engineers are presented.

A.2 Geotextile Design Charts

The Corps of Engineers have developed design charts for determining the stability number (N) and geotextile strength (Tf) required for slope stability [6]. Figure A.1 is a flowchart which describes the process necessary to determine the required geotextile strength. Figures A.2 and A.3 are design charts 1 and 2 respectively.
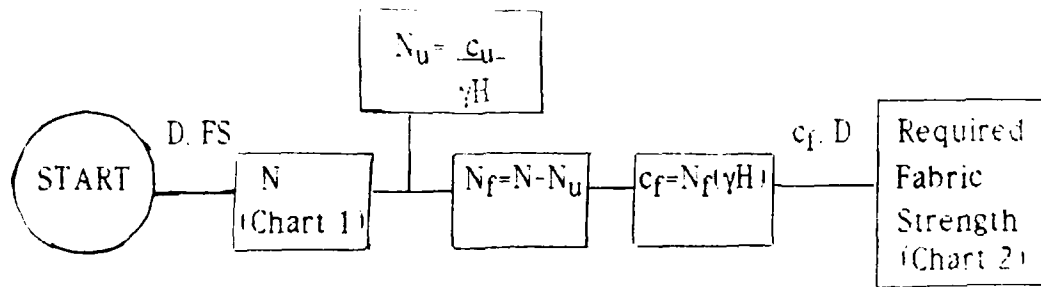
$$N = \frac{c_u + c}{\gamma H} = \frac{c_u}{\gamma H} + \frac{c_f}{\gamma H} = N_u + N_f$$

$$N_f = N - N_u$$

$$c_f = N_f(\gamma H)$$

where

N = stability number for combined contributions from soil and geotextile

N_u = component number for soil cohesion. c_u

N_f = component number for geotextile cohesion. c_f

c_u = unit cohesion of soil. ksf

c_f = unit cohesion of geotextile. ksf

Figure A.1 Flowchart and Description of Basic Definitions for Dimensionless Geotextile Design Charts 1 and 2
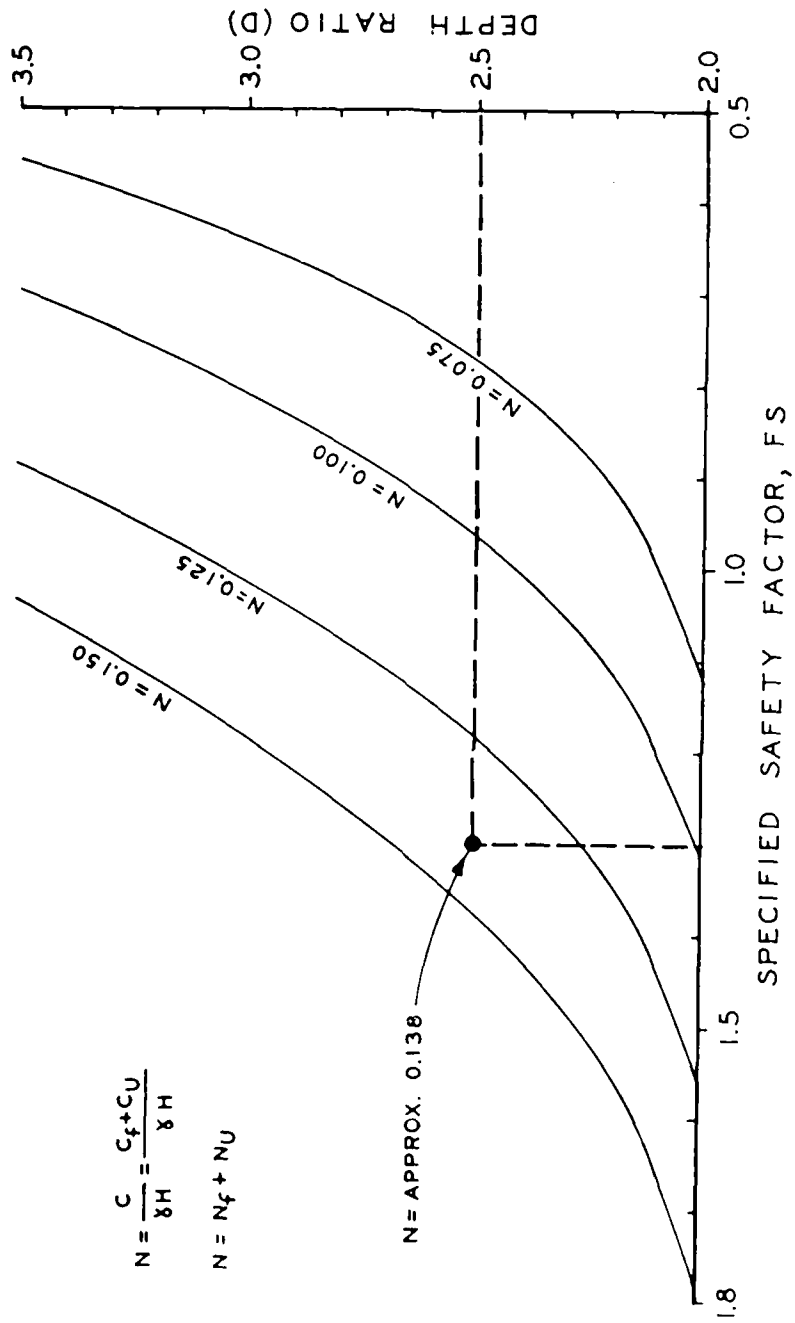
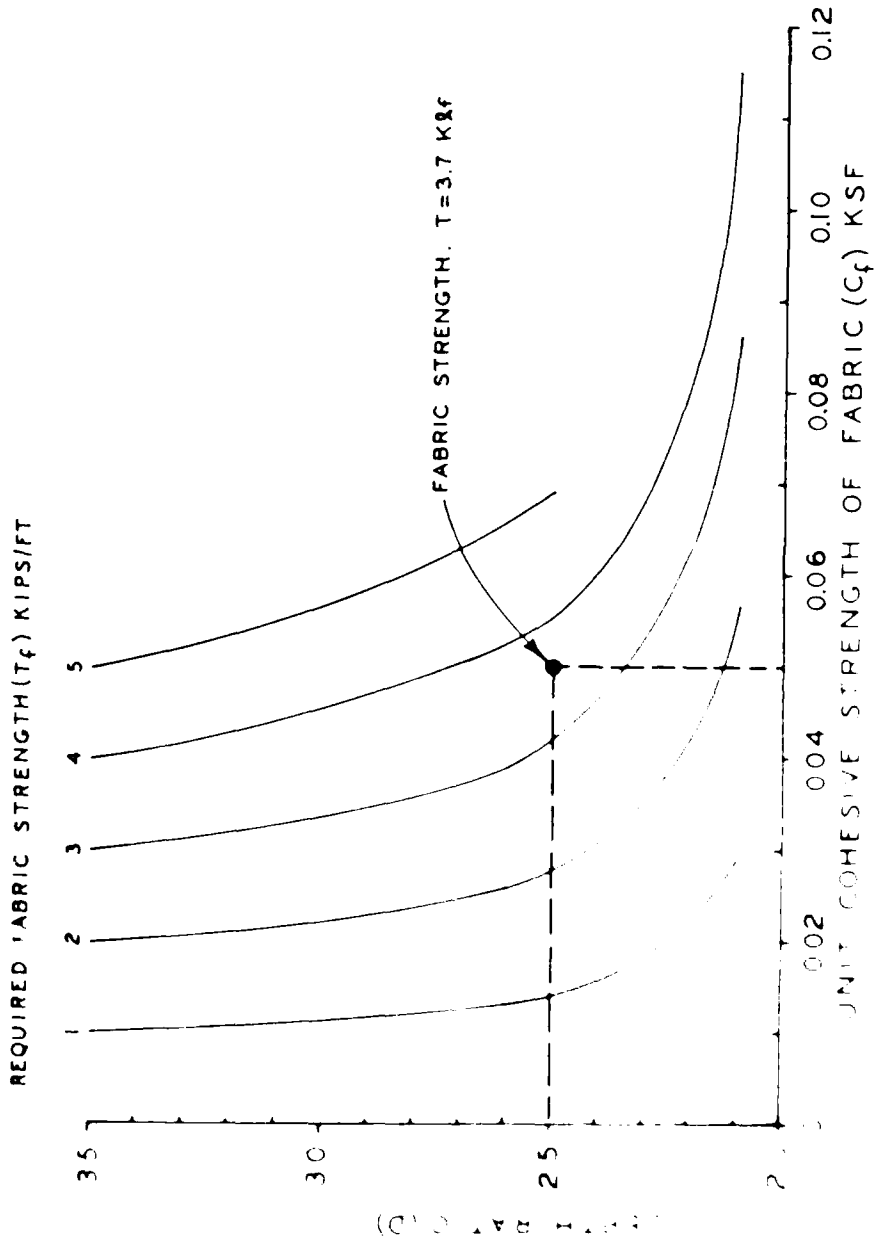**Figure A 2**   Design Chart 1 for Determining Stability Number, N

$$N = \frac{c}{\gamma H} = \frac{c_f + c_u}{\gamma H}$$

$$N = N_f + N_u$$

N = APPROX. 0.138

Figure A.3   Required Fabric Strength in terms of Fabric Strength, T_f

Appendix B
Preliminary Model Development-
Finite Element Method

B.1 Introduction

In this appendix preliminary studies carried out by the author to develop finite element models for the embankment of interest are presented and discussed. The studies involved both linear elastic and linear elastic-plastic models.

B.2 Linear Elastic Model

The initial finite element analyses were conducted using a linear elastic model. This was done to roughly check behavior and to develop some model parameters.

The initial mesh is shown in Figure B.1. Twenty-four elements, type CPE4 were used to model the embankment. The soil was assumed to be homogeneous. Properties corresponding to the upper soil and clay layer were used for all elements (see Table 5.2).
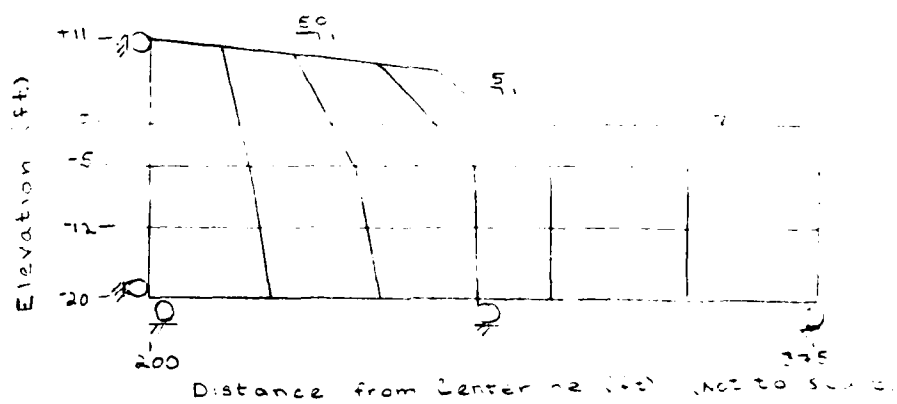
Figure B.1 Initial Mesh- Linear Elastic Model

Plane-strain conditions were assumed for planes perpendicular to the longitudinal axis of the embankment (see section 4.5.2). The conditions at the left vertical boundary and base boundary were represented by roller supports. The right boundary was unrestrained.

The loads applied to the mesh were those associated with the weight of the soil and hydrostatic pressure due to the water surrounding the embankment slope.

With the above items identified, a linear elastic analysis was conducted. In the linear elastic analysis, the full gravity load was applied at one time.

The results of the linear elastic analysis indicated that changes were required in the mesh and boundary conditions. The elements along the embankment slope were judged to be excessively deformed for adequate estimates of behavior. These elements were modified for future analyses. This was accomplished by redefining the shape of the elements (see Figure B.3).

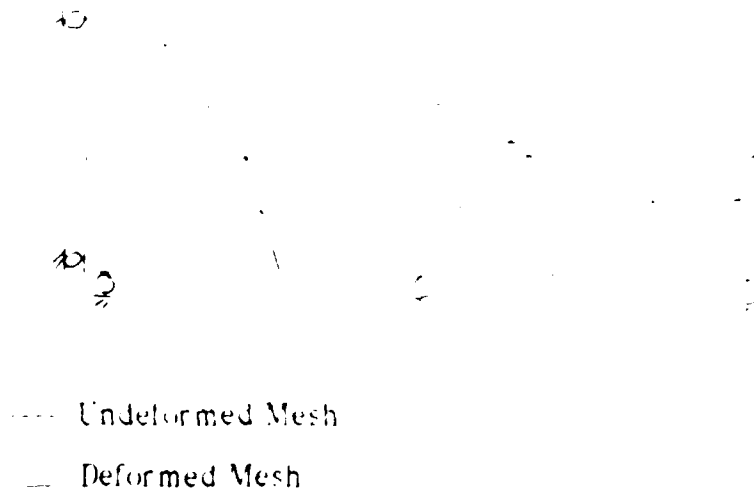—— Undeformed Mesh

— Deformed Mesh

Figure B.2 Displacements Elastic Model

B.3 Linear Elastic Plastic Models

The initial linear elastic plastic model used for finite element analyses (Figure B.3) was based on the linear elastic model discussed

The displacement and traction were assumed to be ... to the embankment ...

Figure B.3 Elastic Plastic Model

The base boundary conditions were initially studied. Finite element analyses were conducted using either roller or fixed boundaries on the vertical sides and base. Also the depth of the base was varied.

First the load applied to the embankment and foundation was due to the weight of the soil. The load was applied as discussed in section 5.3.1. Then a hydrostatic pressure was applied along with the weight of the soil along the surface of the embankment and surrounding foundation soil.

To check the results obtained using the models, comparison studies were carried out. The models described above represent ... ... Estimates for the factors of safety for such embankment slopes can also be obtained using stability number charts such as those provided by Sowers [28] or Terzaghi and Peck [31]. These charts are often used to estimate the factors of safety of slopes. These charts were used to obtain results for comparison with results obtained using the finite element method.

The results obtained from the initial finite element analyses are shown in Table B.1. Additionally, factors of safety estimated using stability number charts are shown. Results are also shown for models which accounted for hydrostatic pressure. In each case, the factor of safety estimated using the finite element method is based on a nonconvergent solution.

	Estimated Factor of Safety					
Depth to Firm Base	F.E.M. with no Hydrostatic Pressure		Stability No. Chart		F.E.M. with Hydrostatic Pressure	
	Roller Base	Fixed Base	T & P*	Sowers	Roller Base	Fixed Base
31 ft	.580	.870	.527	.534	.467	.981
71 ft	.392	.587	.402	.408	.500	.737
Infinite	--	--	.383	.386	--	--

* Terzaghi and Peck

Table B.1 Factors of Safety Estimated using Finite Element Method and Stability Number Charts

The factors of safety estimated using the finite element models with roller supports at the base and no hydrostatic pressures closely approximate the factor of safety estimated using the stability number chart and assuming infinite depth to firm base. Thus, it was felt that the roller supports allowed the best overall representation of the failure of the slope.

The increase in the estimated factor of safety caused by the addition of hydrostatic pressure was consistent with expected behavior. The hydrostatic pressure on the slope face was expected to have a stabilizing effect by providing a moment which would partially counterbalance the moment due to the weight of the embankment.

The finite element model with hydrostatic pressure was further refined to model two and three layers of foundation soil. The lower layers were assigned greater strengths. The properties associated with the middle silt and clay and lower silt and clay layers (see Table 5.2) were used to describe the lower layers of the model. The thicknesses of these layers corresponded to thicknesses found through field testing.

In all cases, the modeling of the layers of the foundation led to increases in the estimated factors of safety. In each case, a nonconvergent solution was obtained. The factor of safety was estimated using the nonconvergent solution. Additionally, in each case, failure was accompanied by the development of a nearly continuous band of yielded elements in the upper foundation layer

... the weakest layer and ... ... layer ... the
layer was consistent with estimates of ... ...
... ... mesh ...

... ... in ... ...
... ...
had ... mesh converted ... ... M ... ...
three foundation layers boundaries ... supports and ... ...
hydrostatic pressure were analyzed ... In each case the ... ...
factor of safety based on a ... ...
approximately 6 ... This indicated that increasing the number of
elements in the mesh from the number originally used had only a
small effect on the estimated factor of safety. Thus the number of
elements used in each mesh for the preceding studies was judged to
be adequate.

The effects of the locations of the side boundaries were also
studied. The left boundaries of both the two and three layer models
were extended to the centerlines of the embankment models. The
right boundaries were progressively extended from 550 ft to 650 ft
from the centerlines. Elements were added to the existing models to
increase the widths. The location of the base boundary was not
changed. The estimated factors of safety did not change from their
original values of 542 (2 layers) and 637 (3 layers). This indicated
that the factor of safety was insensitive to an increase in width of the
model.

The effects of the location of the base boundaries were studied. Using the two and three layer models with the left boundaries located at the centerlines and the right boundaries located 560 ft from the centerlines, the depths of the base boundaries were increased in steps a total of 25 ft. Depth was increased by means of additional elements. The increases in depth resulted in increases in the estimated factors of safety of about 6%. This indicated that additional increases in depth to firm base would result in modest increases in the factor of safety. Modeling the remaining two layers of foundation for a total of five soil layers indicated a depth to firm base specified as 59 ft below mean water level provided adequate results.

Based on the above discussed studies, a finite element model was specified for the embankment. Symmetry was assumed about the centerline of the embankment. Plane strain conditions were specified. The model was specified to have roller supports along the vertical and base boundaries. The width of the model from the centerline of the embankment to the right boundary was specified as 560 ft. The thickness of the model was 74 ft at the centerline and 54 ft in front of the slope. Loadings due to the weights of the soil layers and water were modeled.

The next area which was studied was the modeling of the embankment fill. Initially the embankment fill was assigned a shear strength of zero. This was done for consistency with the Corps of Engineers model. This assumed the layers of the embankment did not have shear strength because of the possibility of tension cracking

However, using the ABAQUS program, we were not able to specify a value of zero for the von Mises failure stress. Thus the embankment fill was given a progressively larger shear strength. Tensile forces developed in the granular layers of the fill, violating the conditions assumed by the Corps of Engineers.

To avoid inconsistencies with the models of the Corps of Engineers, the embankment layers were replaced with a surcharge load. The use of a surcharge load was more consistent with their models because the surcharge basically represented a net applied moment without the addition of a resisting moment.

Once the studies described above were conducted, a second study was conducted to determine the effects of the number of elements. This refinement was done in an attempt to obtain more accurate finite element solutions. Each model was loaded in an attempt to obtain a nonconvergent solution. The initial mesh consisted of 120 elements. Even at four times the loading due to gravity, a non convergent solution was not obtained. Analyses using finer meshes of 455 and 1610 elements were conducted. Again, in each case, nonconvergence was not observed even at multiple levels of gravity loading. As discussed in section 5.4.1, studies were made of the number of failed elements and displacements as functions of the level of gravity load. In general within each mesh the same area failed and displacements amongst the meshes were similar. From these analyses, it was judged that the mesh consisting of 455 elements would provide

adequate results. It was judged that surcharge loading effected the analyses such that a nonconvergent solution was not obtained.

As discussed in section 5.4.1, the above discussed study also lead to the development of a method for estimating a failure load. A distinct failure surface was not observed in the results from any of the analyses. It was judged that since a continuous band of yielded elements did not exist a distinct slip surface did not develop. As a result, a yield criteria was selected to define failure. A study of the yielded elements was conducted on the solutions obtained using the 120 and 455 element meshes. Yielding of an element was said to occur if the stresses at each of the integration points of the element satisfied the criterion of Equation 4.10 to within 2%. In each model, at 100% of the gravity load, a nearly continuous band of yielded elements was observed across the face of the slope in the upper silt and clay layer. The load for which such a condition developed was considered to be the failure load.

In all finite element analyses conducted, under load, the centerline side of the mesh dropped while the side in front of the slope rose. This behavior is the basic overall response anticipated. However, in an actual embankment slope the soil far in front of the slope would not be expected to feel the effects of the embankment load. Without further research, the author cannot give a definite reason for the observed rise in the far field. This behavior may have resulted from the combination of the large horizontal reaction forces that developed on the vertical boundaries in response to the

embankment load and the roller supports along the base. Also, smaller elements directly under the slope may lead to results which better represent expected behavior.

The addition of the geotextile was modestly studied. The geotextile was modeled as a thin, one dimensional, tension only element. The properties specified for the geotextile are shown in Table 5.3.

The geotextile elements were placed on top of the upper silt and clay layer. The geotextile was specified to extend from the centerline of the model to a distance of 48 ft beyond the edge of the embankment slope.

It was specified that no slip could occur between the geotextile elements and the soil elements. This was accomplished by specifying the nodes representing the geotextile elements to be common to the upper nodes of the elements representing the upper silt and clay.

The boundary of the geotextile at the centerline of the model was represented as a vertical roller. The boundary at the other end of the geotextile was specified as free.

The same loads that were applied in the case of the unreinforced embankment were applied in the case of the reinforced embankment. As in the unreinforced model, a nonconvergent solution nor distinct failure surface was obtained. As a result a yield criteria, similar to the one used for the unreinforced embankment, was selected to define failure.

References

1. Andrawes, K., and Mc...... n, A. "The Finite Element Method of Analysis Applied to Soil Geotextile..... ems." Proceedings Second International Conference of Geotextiles, Las Vegas, Nevada, Vol. III, 1982, pp. 695-700.

2. Bishop, A.W., "The Use of the Slip Circle in the Stability Analysis of Slopes." *Geotechnique*, Vol. 5, 1955, pp. 7-17.

3. Bowles, J. E., *Foundation Analysis and Design*, 3rd ed., McGraw-Hill Book Co., New York, N.Y., 1982.

4. Craig, R. F., *Soil Mechanics*, 2nd ed., Van Nostrand Reinhold Co. Ltd., London, UK, 1978.

5. Frohlich, O. K., "General Theory of Stability of Slopes." *Geotechnique*, Vol. 5, 1955, pp. 37-47.

6. Fowler, J., *Design, Construction and Analysis of Fabric-Reinforced Embankment Test Section at Pinto Pass, Mobile, Alabama*, Technical Report EL-81-7, U.S. Army Engineer Waterways Experiment Station, Vicksburg, Miss., 1981.

7. Fowler, J., "Theoretical Design Considerations for Fabric-Reinforced Embankments." Proceedings Second International Conference of Geotextiles, Las Vegas, Nevada, Vol. III, 1982, pp. 665-670.

8. Hibbitt, Karlsson and Sorensen, *ABAQUS User's Manual*, Version 4, Hibbitt, Karlsson and Sorensen, Inc., Providence, R. I., 1982.

9. Higdon, A., Ohlsen, E. H., Stiles, W. B., Weese, J. A., and Riley, W. F., *Mechanics of Materials*, 3rd ed., John Wiley and Sons, Inc., New York, N.Y., 1976.

10. Hoeg. K. "Finite Element Analysis of Strain Softening Clay,"
    Journal of the Soil Mechanics and Foundations Division
    Proceeding of the American Society of Civil Engineers Vol. 98
    SM 1, 1972, pp. 43-58.

11. Huang, Y. H., *Stability Analysis of Earth Slopes* 1st ed., Van
    Nostrand Reinhold Co., New York, N.Y., 1983.

12. Jewell. R. A., "A Limit Equilibrium Design Method for Reinforced
    Embankments on Soft Foundations," Proceedings Second
    International Conference of Geotextiles Las Vegas, Nevada, Vol.
    III, 1982, pp. 671-676.

13. Jones. C. J. F. P., *Earth Reinforcement and Soil Structures* 1st ed,
    Butterworths, Boston, MA, 1985.

14. Koerner. R. M., *Designing with Geosynthetics* 1st ed., Prentice-Hall,
    Englewood Cliffs, N.J., 1986.

15. Lambe, T. W., *Soil Testing for Engineers* John Wiley and Sons,
    Inc., New York, N.Y., 1951.

16. Lo, K. Y., and Lee C. F., "Stress Analysis and Slope Stability in
    Strain-Softening Materials," *Geotechnique* Vol. 23, No. 1, 1973,
    pp. 1-11.

17. Leshchinsky, D., and Reinschmidt, A. J., "Stability of Membrane
    Reinforced Slopes," *Journal of Geotechnical Engineering* ASCE
    Vol. 111, No. 11, 1985, pp 1285-1300.

18. *Mirafi Products for Construction Applications*, Mirafi Inc.,
    Charlotte, N.C., 1984.

19. *Mirafi High Performance Geotextile, Case History, Project
    Washington National Airport Washington, D.C.* TCH-10-1-85,
    Mirafi Inc., Charlotte, N.C., 1984

22. M[...]
[...]
[...]

[...]

[...]

23. [...]
[...]
[...] Las Vegas, Nevada [...]

24. [...]
[...] New [...] [...]

24. Reddy [...]
McGraw-Hill Book [...] New York, N.Y. [...]

25. Rowe P.K. Reinforced embankment [...]
Journal [...] technical Engineering ASCE
No 2 1984 pp 23 24[...]

26. Rowe K.E. The Analysis of an Embankment Constructed on a
Geotextile Proceedings Second International Conference
Geotextiles Las Vegas Nevada Vol III 1982 pp 677 682

27. Snyder M.R. Design Notes and Project Report Washington
National Airport U.S Army Corps of Engineers Baltimore District
1982

28. Sowers G.F. *Introductory Soil Mechanics and Foundations
Geotechnical Engineering* 4th ed MacMillan Publishing Co Inc
New York, N.Y. 1979

29. Stevenson P. Fabric-Reinforced Embankment Provides Airport
Runway Safety Modification *Geotextile Fabrics Report* Spring
1984 pp 4-8

... os Fibers ... ... Centerless Phillips Fibers
... ... 12

... Handbook ... ... s Engineering Practice
... Wiley and Sons ... New York, N.Y. 1967

... ... and Remembrances in Civil
... ... ed ... Wiley and Sons Inc. New York, N.Y.
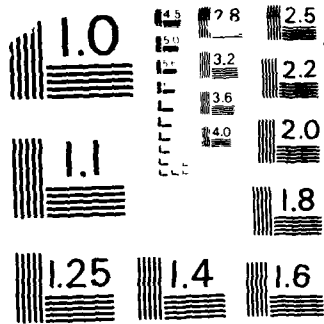
Vita

Deborah L. Nykyforchyn was born in Baltimore, MD on July 15, 1953. She is a 1974 graduate of Towson State University with a Bachelor of Science Degree in Mathematics and Secondary Education and a 1980 graduate of Auburn University with a Bachelor of Science Degree in Civil Engineering. She is currently a captain in the U.S. Army Corps of Engineers. She attended The Johns Hopkins University under the U.S. Army's Top 5% Advanced Degree Program. She is a member of Tau Beta Pi, Chi Epsilon and The Society of American Military Engineers. She is an Engineer-in-Training. She is married to Richard F. Kearney and has one child, Elizabeth Ann.

END

DATE

FILMED

APRIL

1988

DTIC